Carboxylate Ion-Pairing with Alkali-Metal Ions for β-Lactoglobulin and its Role on Aggregation and Interfacial Adsorption

Frank R. Beierlein[a,b] *and Timothy Clark**[,a,b,d]

Björn Braunschweig[b,c] *Kathrin Engelhardt,*[c] *Lena Glas*[c] *and Wolfgang Peukert*[b,c]

[a] Computer-Chemie-Centrum and Interdisciplinary Center for Molecular Materials, Friedrich-Alexander-Universität Erlangen-Nürnberg, Nägelsbachstr. 25, 91052 Erlangen, Germany

[b] Cluster of Excellence Engineering of Advanced Materials, Friedrich-Alexander-Universität Erlangen-Nürnberg, Nägelsbachstr. 49b, 91052 Erlangen, Germany

[c] Institute of Particle Technology (LFG), Friedrich-Alexander-Universität Erlangen-Nürnberg, Cauerstraße 4, 91058 Erlangen, Germany

[d] Centre for Molecular Design, University of Portsmouth, King Henry Building, King Henry I Street, Portsmouth PO1 2DY, United Kingdom

* To whom correspondence should be addressed.

Supporting Information

1. Illustrations of monomer conformations and the different dimers investigated
2. Sample preparation for SFG spectroscopy and ellipsometry
3. Detailed discussion of the SFG spectra
4. Detailed views of the different dimers investigated in the MD study
5. Computational details of monomer, dimer and thermodynamic integration simulations
6. Minima in the radial distribution functions used to define first and second coordination shells (monomer simulations)
7. Radial distribution functions of M^+ around Asp and Glu carboxylate oxygens (monomer simulations)
8. Radial distribution functions of Cl^- around Lys ammonium and Arg guanidinium nitrogens (monomer simulations)
9. Illustrations of the ion distributions in the monomer simulations
10. View of the water environment around a carboxylate pair with and without coordinated cation
11. Radii of gyration as obtained from monomer simulations
12. Illustrations of the ion distributions and the structures in the dimer simulations
13. RMSDs, radii of gyration and distances as obtained from the dimer simulations
14. Gradients and integrated perturbation free energies as obtained from the thermodynamic integration calculations (salt solution without protein and with monomer or dimer)
15. RMSDs, radii of gyration and distances as obtained from the thermodynamic integration simulation of the dimer
16. Illustration of ion distributions and structures in the thermodynamic integration simulation of the dimer
17. Protein diffusion coefficients
18. Details and results of the coarse-grained simulations
19. Hypothetical arrangement of BLG monomers at the air-water interface

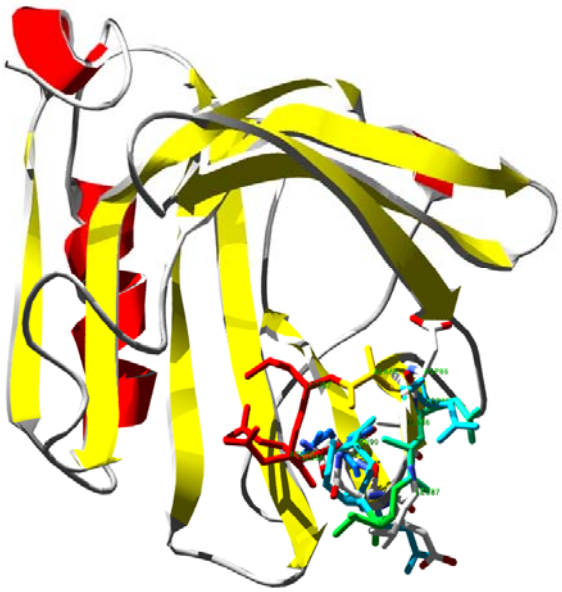

Figure S1. Conformations of loop EF (residues 85-90) in BLGA. CPK: 2BLG (pH 8.2), orange-red: 3BLG (pH 6.2), green-blue: 1BSY (pH 7.1).[1] Images were created using Swiss-PDB-Viewer[2,3] and Pov-Ray.[4,5]

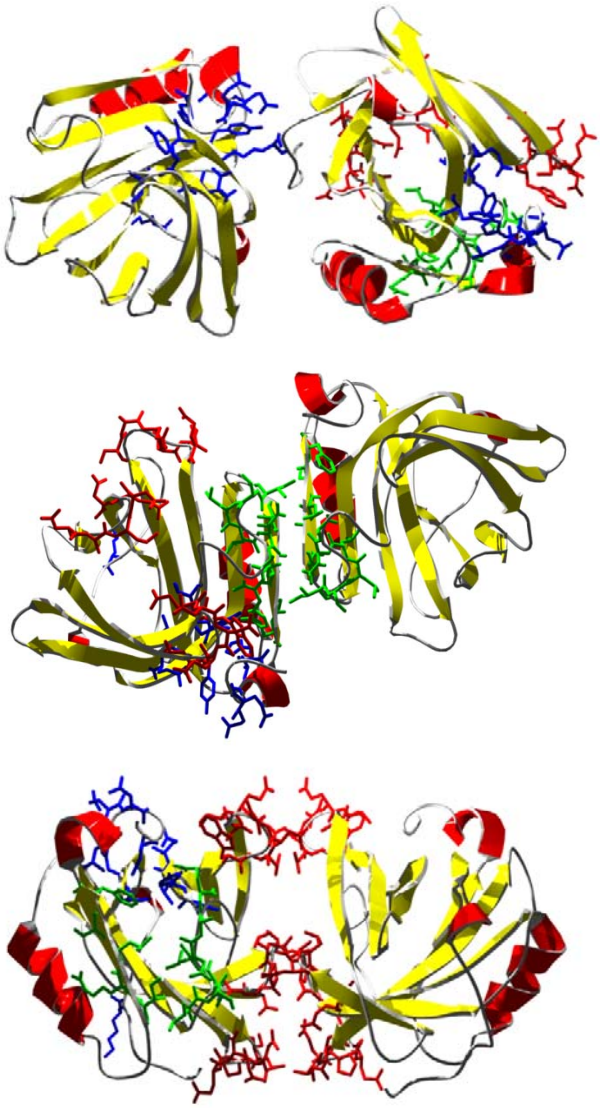

Figure S2. Dimers connected by the "lock-and-key" (above), "dimer" (middle) and "loop" (below) interfaces, based on PDB structure 3BLG.[1] Dimers in cartoon representation with residues forming contacts as colored sticks (blue: "lock-and-key", green: "dimer", red: "loop interface"). For each dimer complex, in one of the monomers, the contact residues of the "other" dimers are additionally drawn, in order to illustrate the position of the interfaces with respect to each other. Images were created using Swiss-PDB-Viewer[2,3] and Pov-Ray.[4,5]

SFG and Ellipsometry Experiments: Sample Preparation

BLG was isolated as described previously[6] and kindly provided by Ulrich Kulozik (Technical University Munich, Germany). 15 μM BLG solutions were prepared by dissolving the dry protein (mixture of BLG A and B) together with salt (concentrations as indicated) in ultra-pure water. The BLG concentration was kept constant at 15 μM for all experiments. Ultra-pure water (18.2 MΩcm; total oxidizable carbon <5 ppb) and LiCl (44762, Alfa Aesar), NaCl (5741.2, Carl Roth) and KCl (104938, Merck Millipore) were used to prepare the solutions. In order to remove possible organic contamination, the necessary glassware for spectroscopic studies was soaked in a mixture of concentrated sulfuric acid (98 %; analytical grade) and NOCHROMIX for at least 24 h and was thoroughly rinsed with ultra-pure water. All measurements were performed at room temperature.

Detailed Discussion of the SFG Spectra

The observed overall changes in SFG spectra are related to electric field induced effects at the interface which can cause substantial changes in the effective electric susceptibility $\chi^{(2)}$. In order to account for possible electric field induced effects, the second-order polarization can be expressed in several (field dependent) terms

$$P_{\omega_{SF}}^{(2)} = \sum \varepsilon_0 \chi_{loc}^{(2)} : E_{\omega_1} E_{\omega_2} + \varepsilon_0 \chi_{dc}^{(2)} E_{\omega_1} E_{\omega_2} + \varepsilon_0 \chi^{(3)} E_{\omega_1} E_{\omega_2} E^{dc} \qquad (S1)$$

where $\chi_{loc}^{(2)}$ is due to a local field independent contribution of the few molecular layers at the interface while $\chi_{dc}^{(2)}$ is due to field induced polar ordering of molecular dipoles at the interface which renders water molecules SFG active as the field induced ordering breaks the inversion symmetry of molecules near the interface and further increases the ordering of molecules directly at the interface (orientation polarization). Thus at high field strengths which should exceed 10^8 V/m this contribution becomes dominant and the SFG intensity in particular from H_2O becomes a function of the electric field.[7] This is also true for the third term ($\chi^{(3)}$) that is caused by an increase in electronic polarization due to the presence of a static electric field E_{dc} at the interface. For that reason O-H bands are very sensitive to the local electric field caused by adsorbed proteins.[8-10] As a consequence, the analysis of SFG spectra in the O-H region can be extremely powerful to study changes in surface charging and molecular structure. In order to analyze SFG spectra each vibrational band is described by a Lorentzian function or in the case of water vibrational bands a Lorentzian (homogeneous broadening) folded with a Gaussian (inhomogenous broadening). The amplitude $A_q = N \int f(\Omega)\, \beta_q(\Omega)\, d\Omega$ and the phase of each band q are directly correlated to the orientation distribution $f(\Omega)$ of interfacial molecules. As the spectral dependence of $\chi_{dc}^{(2)}$ and $\chi^{(3)}$ is identical we will simply describe the sum of these

contributions by a field dependent effective second-order susceptibility. For that reason, changes in strength and orientation of E_{dc} can be monitored in addition to changes in number density N and molecular orientation e.g. due to different adsorption geometries such as protein adsorption in its monomeric or dimeric form.

As a consequence it is possible to attribute the decrease in SFG intensity of O-H stretching bands with increasing ionic strength to a decrease in interfacial electric field. The latter can be caused by an increase in charge screening with increasing ionic strength and by ion specific effects that modify the electric field at the interface in addition to charge screening. While the reduction in O-H intensity can be explained by a change in surface charging conditions, the observed additional change in spectral shape in the frequency region of 3000 – 3200 cm^{-1} as already reported in the main text, is possibly due to a change in molecular orientation at the interface of either interfacial H_2O or BLG molecules.

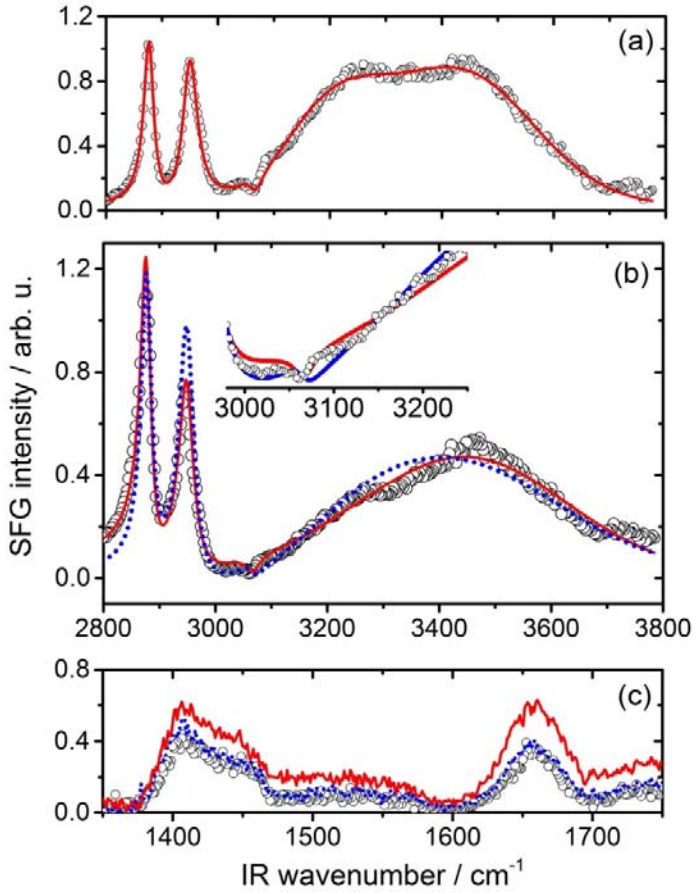

Figure S3. Vibrational SFG spectra for β-lactoglobulin modified air-water interfaces with a bulk electrolyte that has a LiCl concentration of (a) 0 and (b) 1.5 M. The spectra were fitted with identical frequencies, amplitudes and bandwidth for the C-H stretching modes, but different O-H amplitudes. In (b) we compare fits where also the phase of C-H modes was kept fixed (dotted blue line) and where the phase was changed by $\pi/2$ (solid red line). (c) SFG spectra in the range of Amide I (~1650 cm^{-1}) and symmetric stretching vibrations of carboxylate side (~1420 cm^{-1}) chains for 1.25 M (red solid line), 0.25 M (blue dotted line) and 0.01 M (open circles) LiCl concentrations.

That is because the intensity of the O-H bands in Figures 3d-f (main text) has not changed to a large extent, the observed changes are inconsistent with a simple decrease in O-H amplitude and it is likely that the relative phase between O-H and C-H bands changes and thus causes the apparent change in spectral shape. Figures 3d-f (main text) provide a more detailed representation of this region at concentrations where the changes are most apparent. As for all salts similar changes occur, we focus on LiCl, the conclusions are, however, analogous for NaCl and KCl salts. Consequently, a change in the phase of either O-H or C-H bands must be taken into account.

In order to further analyze this behavior, we have fitted our spectra with model functions which have been described above. In order determine which parameters (amplitudes and phases) change as a function of ionic strength, we have first fitted the spectrum at 0 M LiCl concentration where we varied amplitudes, phases and the center frequencies of each vibrational band (Figure S3 (a)). Starting from these parameters we modeled the SFG spectrum at 1.5 M LiCl which has similar shape as the other spectra at ionic strengths between 0.1 and 1.5 M (Figure 3, main text). In Figure S3 (b) we show fits to the SFG spectrum at 1.5 M which are based on the parameters of the fit to the spectrum at 0 M LiCl concentration. A close inspection of Figure S3 (b) reveals that it is not sufficient to allow only the amplitudes of the O-H stretching modes as free parameters, but it is necessary to include an additional phase change of all C-H bands by $\pi/2$. Otherwise, the difference between the fit and the experimental data is quite substantial in particular in the C-H region (2800 – 3100 cm^{-1}). We recall that the phase of a vibrational band in SFG spectra is directly correlated to the molecular orientation of interfacial species that give rise to the vibrational band. For that reason the observed phase change of BLG can be attributed to a change in protein net orientation by 90°. In order to address the possible

change in protein orientation in more detail, we have recorded SFG spectra in a spectral region where stretching vibrations (~1620 cm^{-1} β-sheets; ~1650 cm^{-1} α-helix; ~1670 cm^{-1} disordered structures) from amide groups located in the protein backbone and symmetric stretching vibrations of carboxylate groups (~1420 cm^{-1}) can be observed. Figure S3 (c) presents SFG spectra in this region for LiCl concentrations of 0.01, 0.25 and 1.25 M. The spectra for LiCl concentrations of 0.01 and 0.25 M are within the scatter of our measurement identical in both shape and intensity, while the SFG spectrum recorded at 1.25 M has higher overall intensity but identical shape. From this comparison we conclude that in this spectral region no changes in the phases of all contributions take place. Therefore, the question arises why there is a phase change for C-H/O-H bands on the one hand and no phase change for Amide I and carboxylate bands on the other hand. The fact that there is a negligible change in shape and intensity for Amide I and carboxylate bands at LiCl concentration <0.25 M indicates the net orientation of the molecular groups contributing to these bands must remain similar to the orientation at low ionic strength.

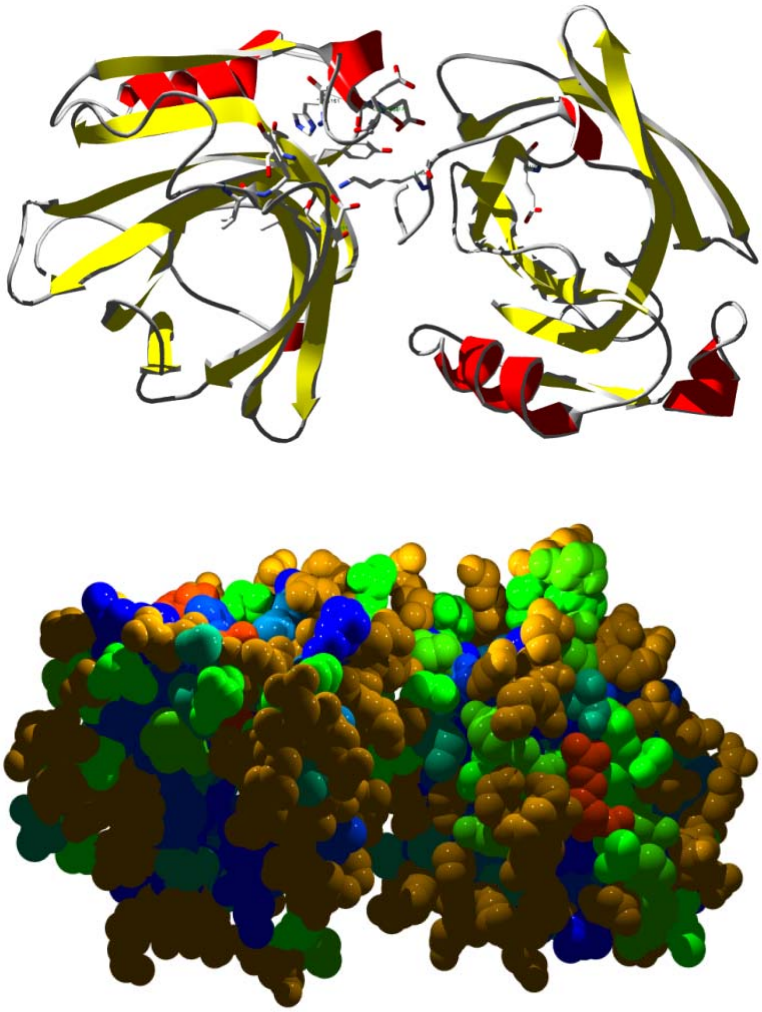

Figure S4. Dimer connected by the "lock-and-key interface", based on PDB structure 3BLG.[1] Above: dimer in cartoon representation with selected residues as sticks. Below: dimer colored according to hydrophobicity (blue = hydrophobic, e.g. Leu, Ile, Val; green: Cys, Phe, Ala, Thr, Gly, Met, Trp, Ser, Tyr, Pro; brown: Gln, His, Lys, Asn, Glu, Asp; red: Arg). Images were created using Swiss-PDB-Viewer[2,3] and Pov-Ray.[4,5]

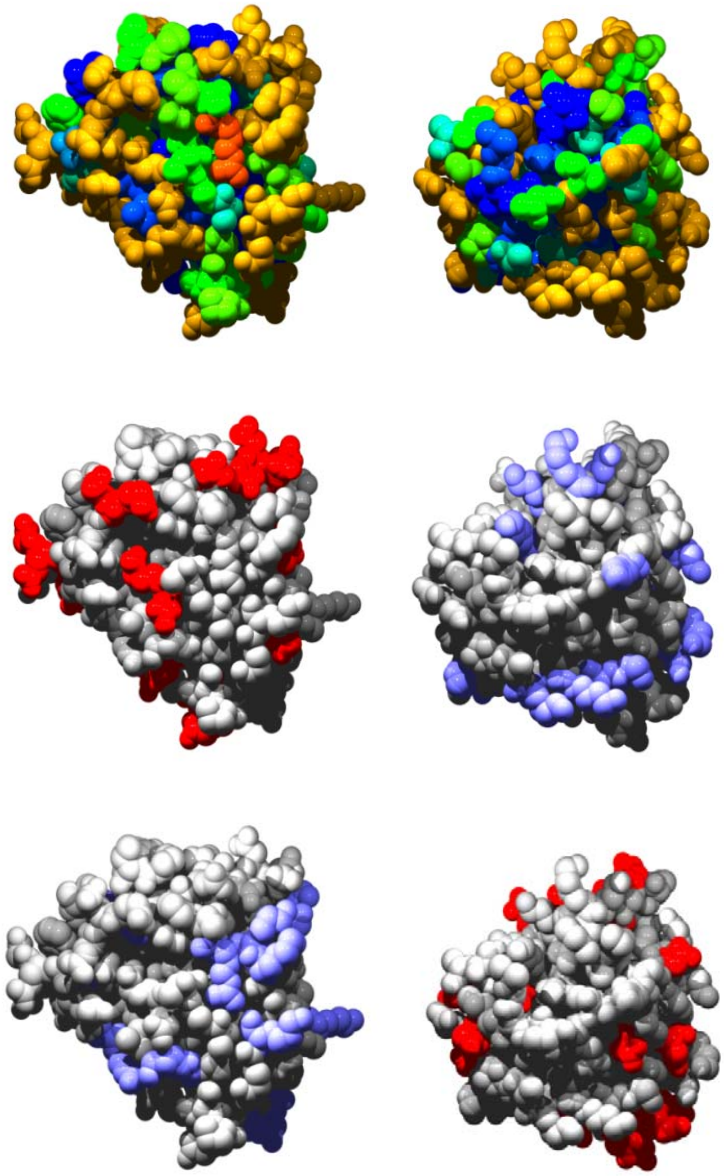

Figure S5. Dimer connected by the "lock-and-key interface", based on PDB structure 3BLG.[1] Above: view of the contact surfaces (monomers rotated for a direct view) colored according to hydrophobicity (blue = hydrophobic, e.g. Leu, Ile, Val; green: Cys, Phe, Ala, Thr, Gly, Met, Trp, Ser, Tyr, Pro; brown: Gln, His, Lys, Asn, Glu, Asp; red: Arg). Middle and below: contact surfaces colored according to charge (negative = red, positive = blue). Images were created using Swiss-PDB-Viewer[2,3] and Pov-Ray.[4,5]

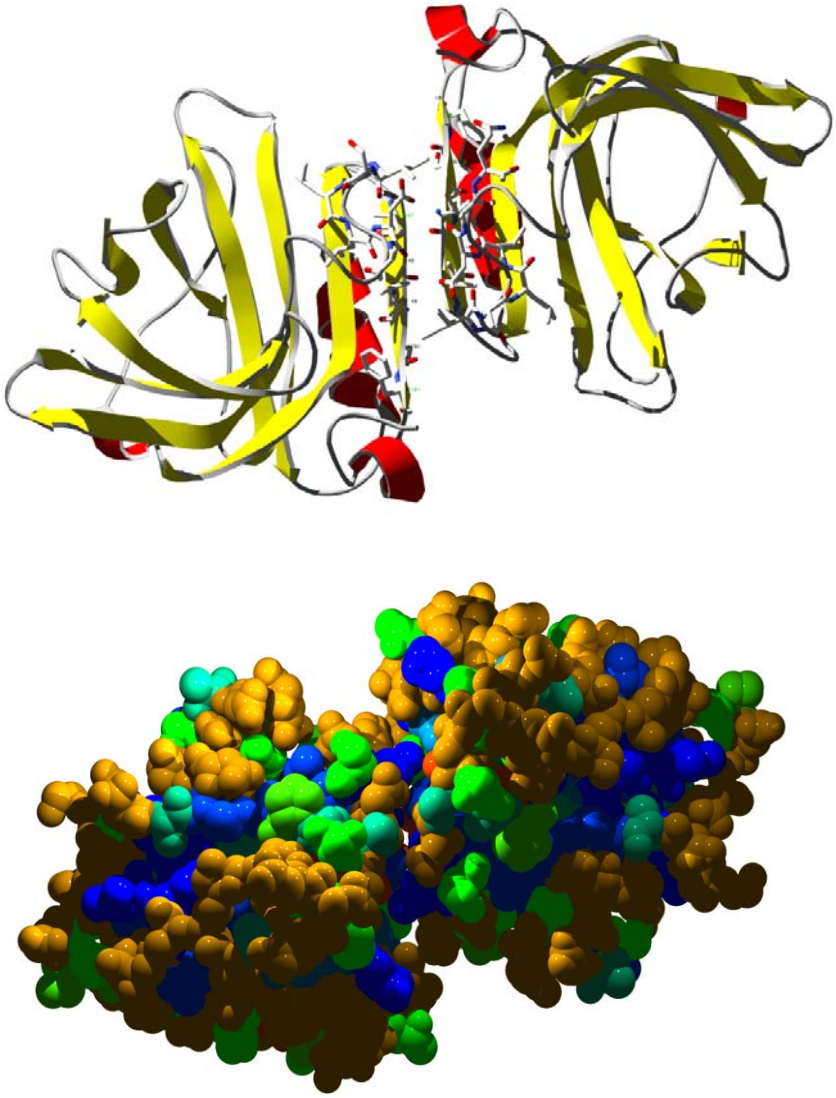

Figure S6. Dimer connected by the "dimer interface", based on PDB structure 3BLG.[1] Above: dimer in cartoon representation with selected residues as sticks. Below: dimer colored according to hydrophobicity (blue = hydrophobic, e.g. Leu, Ile, Val; green: Cys, Phe, Ala, Thr, Gly, Met, Trp, Ser, Tyr, Pro; brown: Gln, His, Lys, Asn, Glu, Asp; red: Arg). Images were created using Swiss-PDB-Viewer[2,3] and Pov-Ray.[4,5]

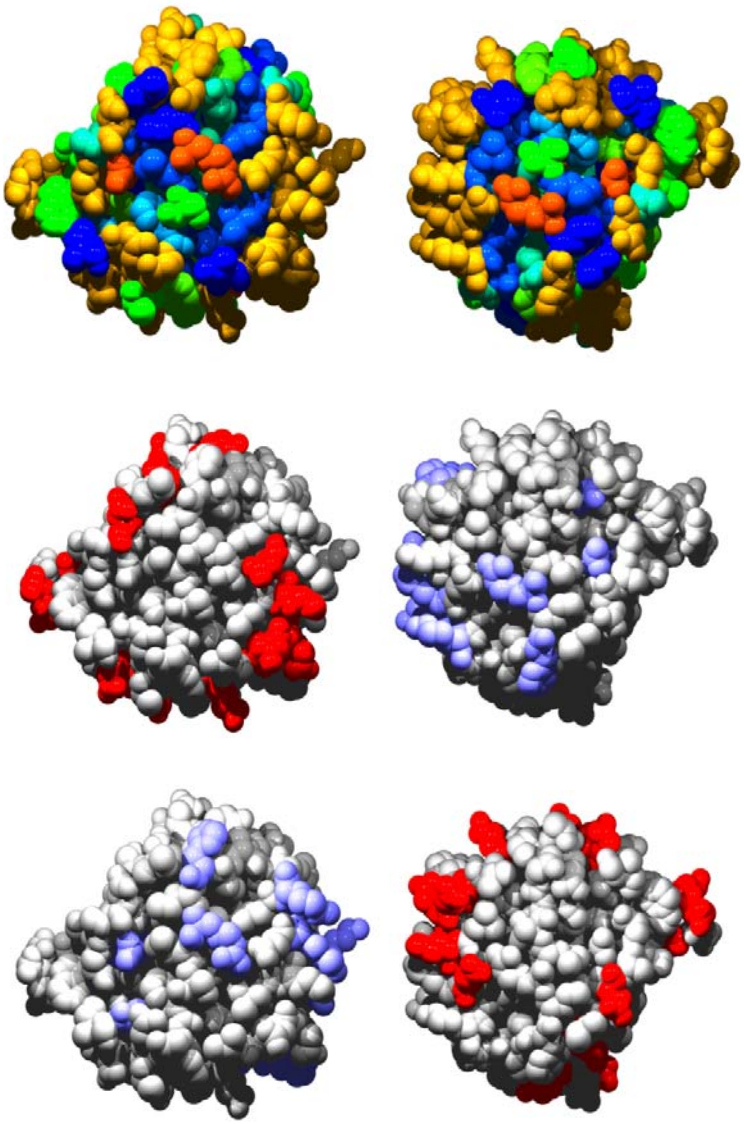

Figure S7. Dimer connected by the "dimer interface", based on PDB structure 3BLG.[1] Above: view of the contact surfaces (monomers rotated for a direct view) colored according to hydrophobicity (blue = hydrophobic, e.g. Leu, Ile, Val; green: Cys, Phe, Ala, Thr, Gly, Met, Trp, Ser, Tyr, Pro; brown: Gln, His, Lys, Asn, Glu, Asp; red: Arg). Middle and below: contact surfaces colored according to charge (negative = red, positive = blue). Images were created using Swiss-PDB-Viewer[2,3] and Pov-Ray.[4,5]

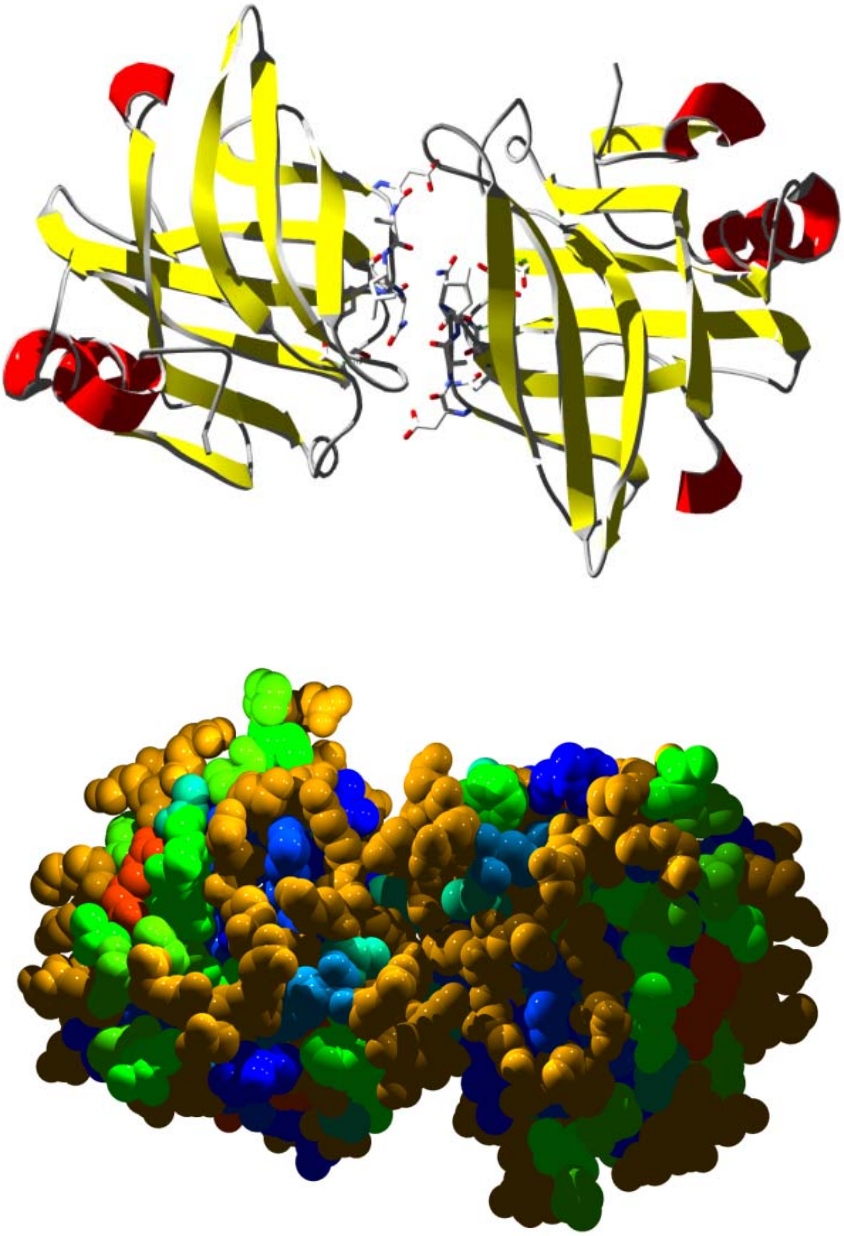

Figure S8. Dimer connected by the "loop interface", based on PDB structure 3BLG.[1] Above: dimer in cartoon representation with selected residues as sticks. Below: dimer colored according to hydrophobicity (blue = hydrophobic, e.g. Leu, Ile, Val; green: Cys, Phe, Ala, Thr, Gly, Met, Trp, Ser, Tyr, Pro; brown: Gln, His, Lys, Asn, Glu, Asp; red: Arg). Images were created using Swiss-PDB-Viewer[2, 3] and Pov-Ray.[4,5]

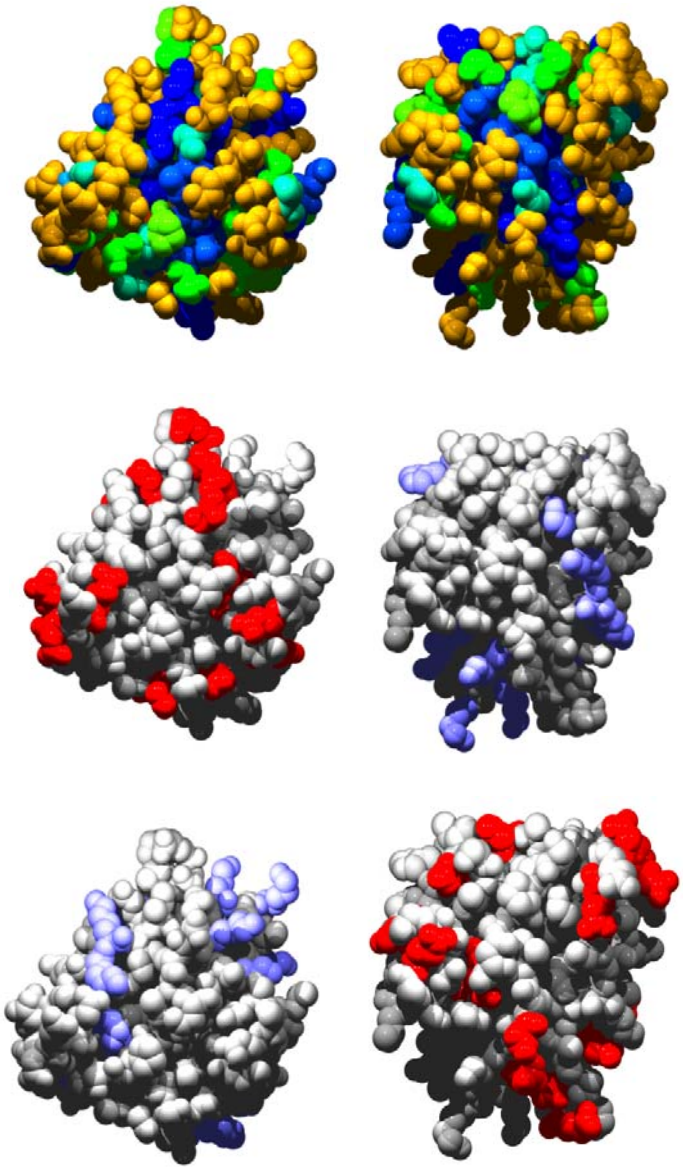

Figure S9. Dimer connected by the "loop interface", based on PDB structure 3BLG.[1] Above: view of the contact surfaces (monomers rotated for a direct view) colored according to hydrophobicity (blue = hydrophobic, e.g. Leu, Ile, Val; green: Cys, Phe, Ala, Thr, Gly, Met, Trp, Ser, Tyr, Pro; brown: Gln, His, Lys, Asn, Glu, Asp; red: Arg). Middle and below: contact surfaces colored according to charge (negative = red, positive = blue). Images were created using Swiss-PDB-Viewer[2,3] and Pov-Ray.[4,5]

Atomistic MD, Monomer Simulations: Computational Details

Initially, 5,000 steps of geometry optimization were performed (500 steps of steepest decent and 4,500 steps of conjugate gradient) using weak restraints (50 kcal mol^{-1} $Å^{-2}$) on the protein atoms, followed by 5,000 steps with 10 kcal mol^{-1} $Å^{-2}$ on the protein main chain atoms. The optimized structures were used as input for Langevin dynamics simulations at 298 K, using a 2 fs time step and a collision frequency of 2 ps^{-1}. Langevin dynamics is the recommended method for temperature control in current versions of the MD software Amber, and is reported to provide better results than e.g. weak-coupling or Anderson coupling. Bonds involving hydrogen were constrained using SHAKE.[11] The distance cutoff for all nonbonding interactions was set to 12 Å. Long-range electrostatics were described by the particle-mesh Ewald method.[12,13] For van der Waals interactions beyond those included in the direct sum, a continuum model correction for energy and pressure was used, as implemented in Amber 12.[14] System heat-up was performed during a 500 ps constant volume (NVT) simulation with weak restraints (10 kcal mol^{-1} $Å^{-2}$) on the protein main-chain atoms. The systems were then simulated for 600.5 ns for the systems containing Na^+ and the K^+, and 100.5 ns for the Li^+ system at constant pressure (NPT) (1 bar, weak pressure coupling, isotropic position scaling, pressure relaxation time 2 ps) without any restraints. Detailed analyses of the ion distribution were performed in the 80.5-100.5 ns interval: First, the following radial distribution functions (RDFs) were determined: M^+ and water oxygen (treated as solvent in ptraj)[15] around carboxylate oxygens of Asp, Glu (solute), M^+ and water oxygen around backbone carbonyl oxygens, chloride ions and water oxygens around cationic Lys ammonium nitrogens and Arg guanidinium (NH1,NH2) nitrogens, water oxygens around M^+, and water hydrogens around chloride. Additionally, we determined the RDFs and the integrals of the RDF bin values for M^+ and Cl^-, respectively, around the center of mass (COM) of

all protein heavy (non-hydrogen) atoms with cpptraj[15] from the Amber14 suite.[16] Distances determined from the minima in the RDFs for the first and second shells of M^+ and water oxygen around carboxylates and backbone carbonyl oxygens, respectively (see Table S1), were then used to calculate the number of contacts between the species, using the ptraj "watershell" command. A similar procedure was chosen to calculate the contacts of Cl^- with the ammonium nitrogen and the guanidinium nitrogens of the positively charged amino acids Lys and Arg. The contact numbers are given in Figure 5 and Table 1 in the main text for the contacts between M^+ and the carboxylate oxygens of individual Asp and Glu residues (Figure 5) and all Asp/Glu residues in the system (Table 1). Mean residence times of ions and water were calculated as described previously.[17-19] Diffusion coefficients were determined for the LiCl system over an interval from 10.5-100.5 ns and for the NaCl/KCl systems from 100.5-600.5 ns (see below). To obtain plots of the total charge of the protein and the surrounding ions as a function of the distance from the protein center of mass, the protein net charge (-5 e at pH 6.2) and the integrals of the RDF bin values of the cations and the anions were used: $Z_{total} = Z_{protein} + Z_{cations} - Z_{anions}$.

Atomistic MD, Dimer Simulations: Computational Details

No aspartate, glutamate or histidine residues were protonated in the structures with loop EF open, and only the glutamates Glh89 of both monomers were protonated in the structure with this loop closed. Histidines His146 of both monomers were treated as "Hid", His161 as "Hie". This protonation state corresponds approximately to a pH of 8.2 according to the pK_a prediction tools. Disulfide bridges were defined as in the monomer case. The total charge of the final dimer was −18 in the case of the structure with loop EF open, and −16 with it closed. The structures were solvated in SPCE[20] water, and Na^+ and K^+ counterions added to each system. Additionally, NaCl/KCl ions were added to achieve an electrolyte concentration of 100.7 mM M^+ ("loop interface", loop closed) and 100.8/101.7/101.8 mM M^+ (loop open, "dimer", "loop", "lock-and-key" interface structures). Metal-ion positions were randomized using Amber 12 ptraj. Ions were treated using Joung/Cheatham[21] parameters (JC), additionally, for comparison, simulations of the "loop interface" structure were repeated with ion parameters given in data set 5 in the paper by Horinek, Mamatkulov and Netz (HN).[22] In the simulation with the latter parameters, the dimer in the Na^+ simulation separated too quickly for our understanding. The well depths for the cations in the HN parameter set are much smaller than in the Joung/Cheatham parameter set, and also the values for $R_{min}/2$ are much larger than the ones used by JC, which more closely resemble ion radii. These parameters seemed to us to be too "weak" for the problem under investigation. MD-simulation parameters were chosen as in the monomer simulations. In the "dimer" and "lock-and-key interface" simulations, a simulation time of 61.5 ns was chosen and detailed analyses were carried out from 41.5 – 61.5 ns. In the case of the "loop interface" structure based on 2BLG (loop open), simulations were propagated until 209.5 ns and detailed analyses were performed

for 101.5-209.5 ns. For the “loop interface” structure based on 3BLG (loop closed), the simulation time was extended to 413.5 ns (analysis interval 101.5-413.5 ns).

Thermodynamic Integration: Computational Details

In order to avoid the problem of a charged system in the "free leg" of the simulations, i.e. the one in which the cations are perturbed into each other in water alone, we used a neutral protein for the TI simulations (i.e., the protein at the isoelectric point). For the monomer, the electrically neutral protein (corresponding to a pH of ca. 4-5) was obtained from PDB structure 3BLG by protonating the following residues: Ash33, Glh44, Glh74, Glh89, Glh114, Glh157, Glh158, Hip146, Hip161. Additionally, a monomer simulation was performed with Glh131 protonated instead of Glh74, which turned out to be too close to the interface in the dimer simulation. In the dimer simulation, residues Ash33, Glh44, Glh89, Glh114, Glh131, Glh157, Glh158 in both monomers were protonated. The initial structure, constructed from PDB code 3BLG and connected by the "loop interface", was slightly modified by pulling the monomers apart by ca. 2.7 Å, thus creating space for bridging cations. The protein was solvated in a truncated octahedral box of SPCE waters, which exceeds the protein dimensions by 10 Å (monomer) and 15 Å (dimer) in each direction. MCl electrolyte ions were then added to obtain an M^+ concentration of 100 mM (monomer: 9 MCl, 101.3 mM; dimer: 40 MCl, 101.12 mM), these ions were not randomized in the simulations with protein present, i.e. the ions were placed in positions with a favorable Coulombic interaction with the protein. For van-der-Waals interactions, a cutoff of 10 Å was used. All other simulation parameters were chosen as in the non-TI-simulations described above. The monomer was pre-equilibrated at $\lambda = 0.0$ (K^+) for 100.5 ns, and at $\lambda = 1.0$ (Na^+) for 60.5 ns to get structural information about the protein at the isoelectric point. Standard MD analyses (not shown) showed that the system was stable and well equilibrated after these times. For Na^+, an average (analysis interval: 30.5 – 60.5 ns) of 3.29 Na^+ ions was found to be coordinated in the first and second coordination shells around deprotonated

Asp and Glu; this number is 2.62 for K^+ (50.5-100.5 ns). The pre-equilibrated monomer system with KCl was then used as starting structure for dual-topology Sander.MPI simulations with Amber12.[14,23] Nine λ-windows (0.1, …, 0.9) were used to represent the transition from K^+ to Na^+. Separate simulation "legs" were established for the "bound" (protein + ions/water) and "free" cases (ions/water). Initial geometry optimization, equilibration and data acquisition were performed at each λ value. For the monomer simulation with Glh74 protonated, equilibration of 5.5 ns was followed by data collection over 10 × 2 ns (5.5-25.5 ns). In the monomer simulation with Glh131 protonated instead of Glh74, we chose a longer equilibration (15.5 ns), and collected gradients of $\langle dV/d\lambda \rangle$ over 10 × 2 ns (15.5-35.5 ns). Numerical integration according to the midpoint rule was used to obtain the perturbation free energies for the individual simulation intervals, gradients for λ = 0.0 and λ = 1.0 were obtained by extrapolating from neighboring λ-values. As precision estimates we used the standard error from consecutive MD runs (batch averaging), which has been shown to agree well with more advanced error analysis in our previous work on DNA base-pair mutations by TI.[24]

In the case of the dimer simulations, no pre-equilibration at λ = 0.0 was performed to avoid any bias on the structure, here, the initial solvated structure with KCl was only geometry optimized (500 steepest descent and 4500 conjugate gradient minimization steps). Then, the system was geometry optimized and equilibrated (5.0 ns) at each λ value (0.1, ..., 0.9). Data acquisition was performed over 40 x 0.5 ns (5.0-25.0 ns.)

Table S1. Minima in the radial distribution functions [Å] that were used to define first and second coordination shells (atomistic MD, monomer simulations).

	M^+/COO^-		WatO/COO^-		M^+/BB-O	WatO/BB-O		Cl^-/Lys-N		Cl^-/Arg-N
	1st	2nd	1st	2nd	1st	1st	2nd	1st	2nd	
WatO (LiCl)			3.18	5.15		3.35	5.45			
Li^+	2.70	5.22			2.26					
Cl^- (LiCl)								4.00	6.40	6.40
WatO (NaCl)			3.18	5.47		3.35	5.48			
Na^+	3.12	5.26			3.30					
Cl^- (NaCl)								4.00	6.40	6.40
WatO (KCl)			3.25	5.54		3.36	5.47			
K^+	3.55	5.50			3.90					
Cl^- (KCl)								4.00	6.40	6.40

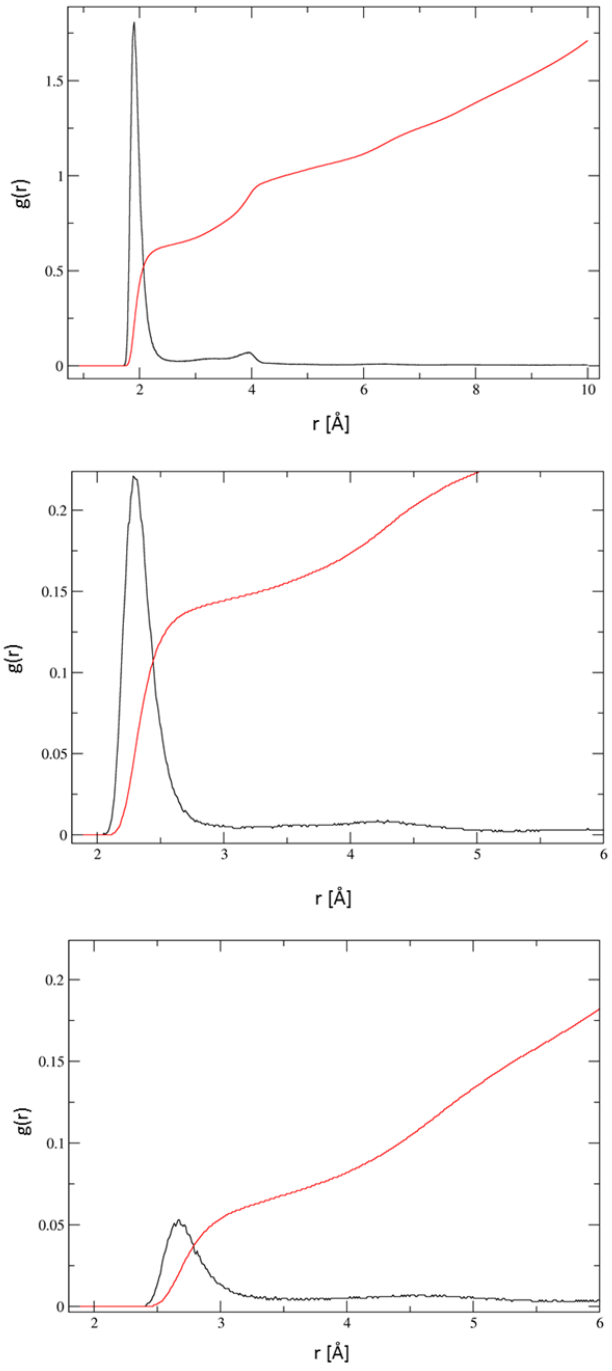

Figure S10. Radial distribution functions (black, integrals: red) of Li^+ (above), Na^+ (middle), K^+ (below) around Asp and Glu carboxylate oxygens (monomer simulations, 100 mM M^+).

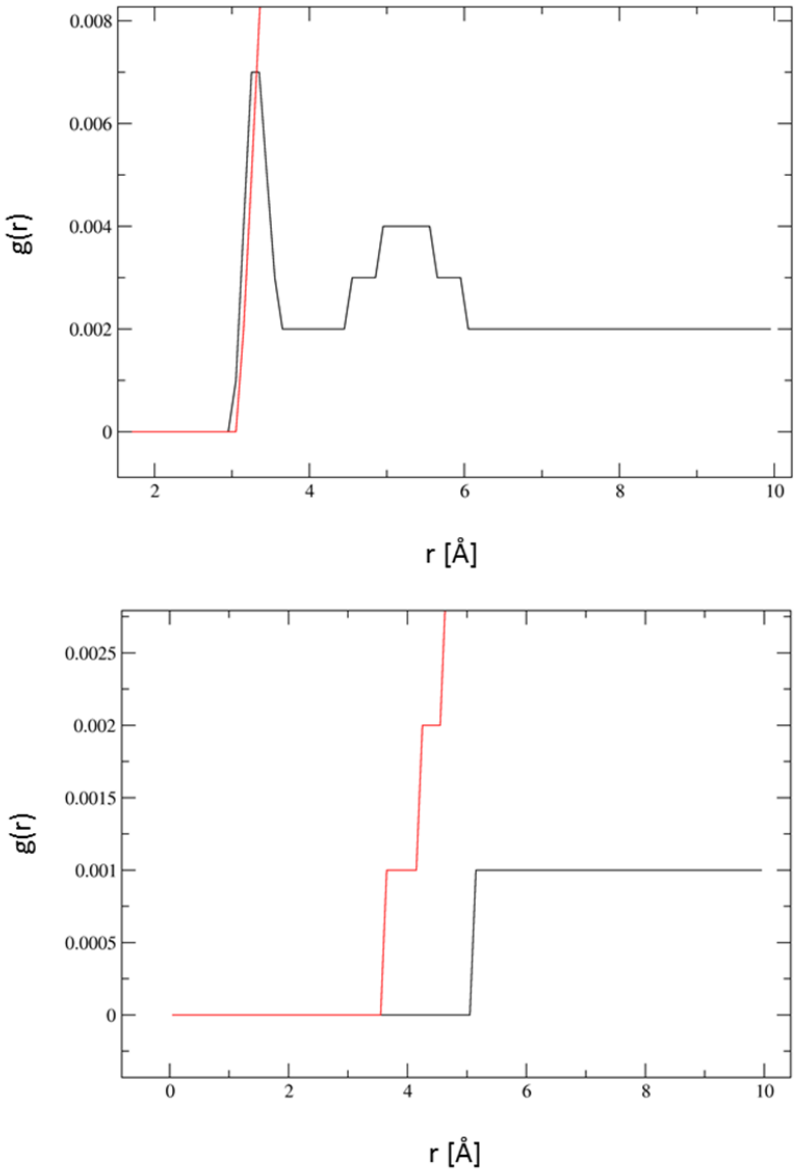

Figure S11. Radial distribution functions (black, integrals: red) of Cl^- around Lys ammonium (above) and Arg guanidinium (NH1/NH2, below) nitrogens (monomer simulation with 100 mM LiCl).

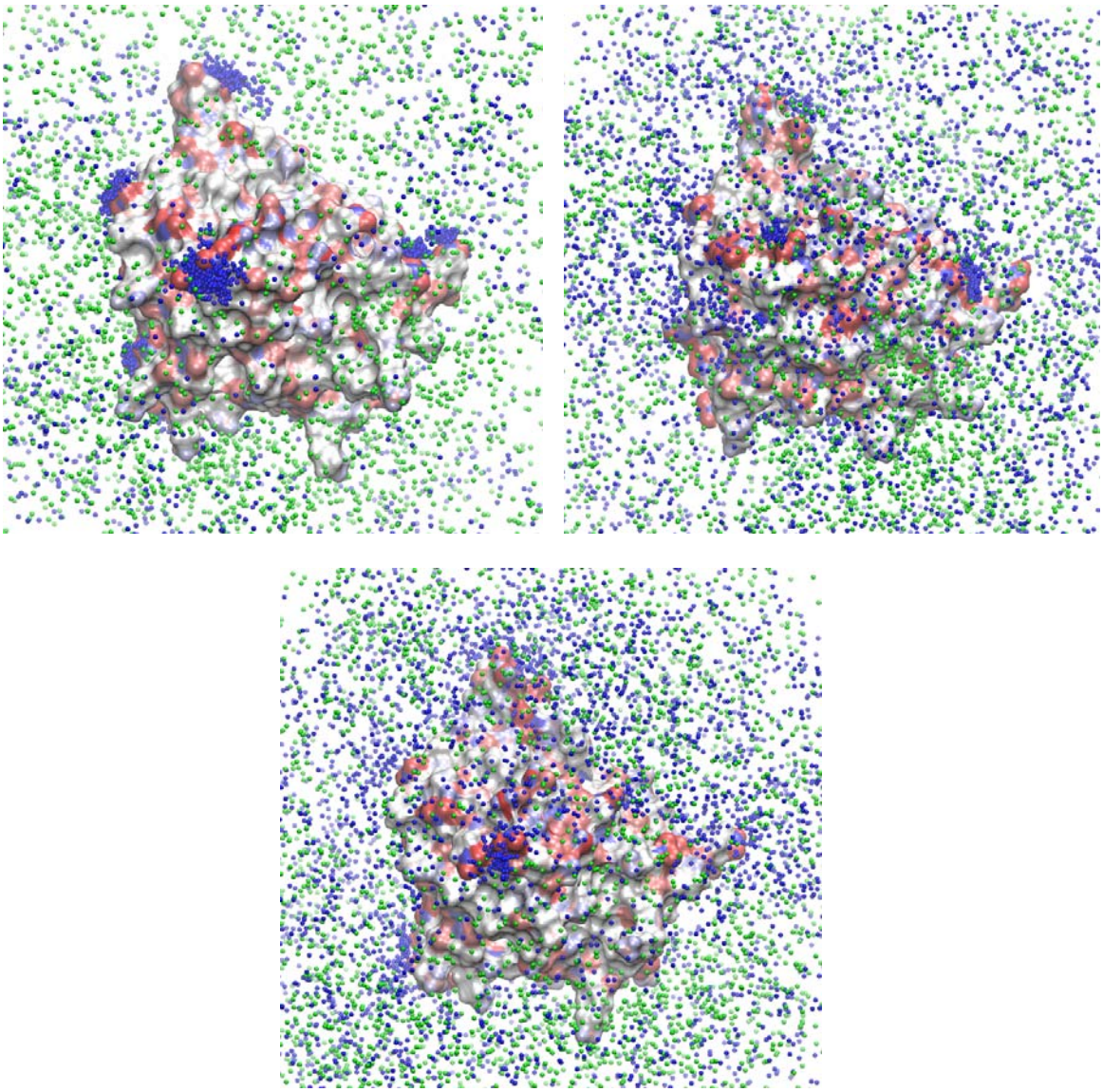

Figure S12. Li^+ (above/left, blue), Na+ (blue, above/right), K+ (blue, below) and Cl^- (green) distribution around a BLGA monomer (solvent accessible surface colored according to charge, red = negative, blue = positive). Simulations with 100 mM LiCl/NaCl/KCl, analysis interval 80.5-100.5 ns, all frames fitted on minimized structure, only every 100th frame for MCl shown for clarity. Figures were created using VMD.[25,26]

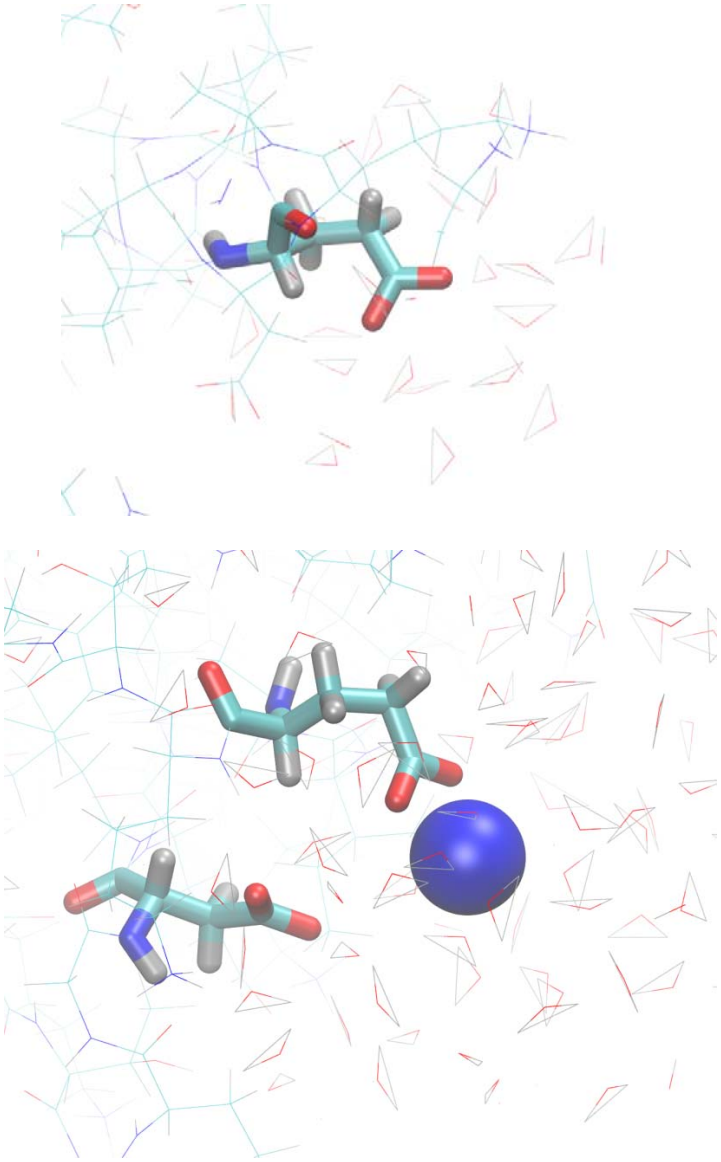

Figure S13. Monomer simulation with 100 mM NaCl, snapshot at 100.5 ns. Water molecules (triangles red/silver) and sodium ion (blue sphere) within 5 Å of Glu134 (sticks, above) and the Asp53/Glu74 pair of residues (sticks, below). Figures were created using VMD.[25,26]

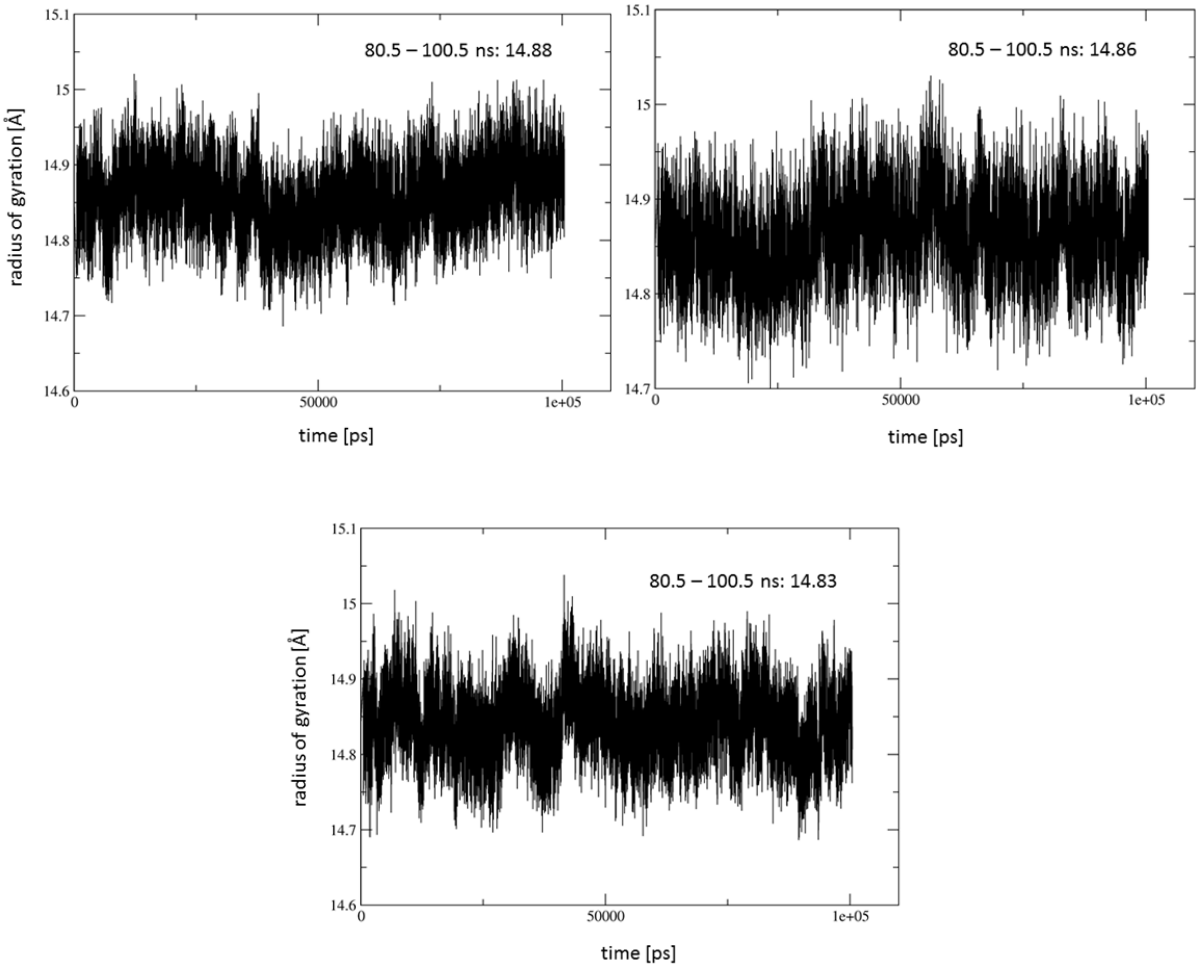

Figure S14. Radius of gyration, calculated for all protein atoms. Above, left: simulations with LiCl electrolyte; above, right: simulations with NaCl; below: simulations with KCl. Data shown for simulations of monomers with loop EF closed (3BLG). Analysis interval: 0.5-100.5 ns, additionally mean values are given for 80.5-100.5 ns, all frames were fitted on the minimized X-ray structure before analysis, electrolyte concentration 100 mM, Joung/Cheatham ion parameters were used.

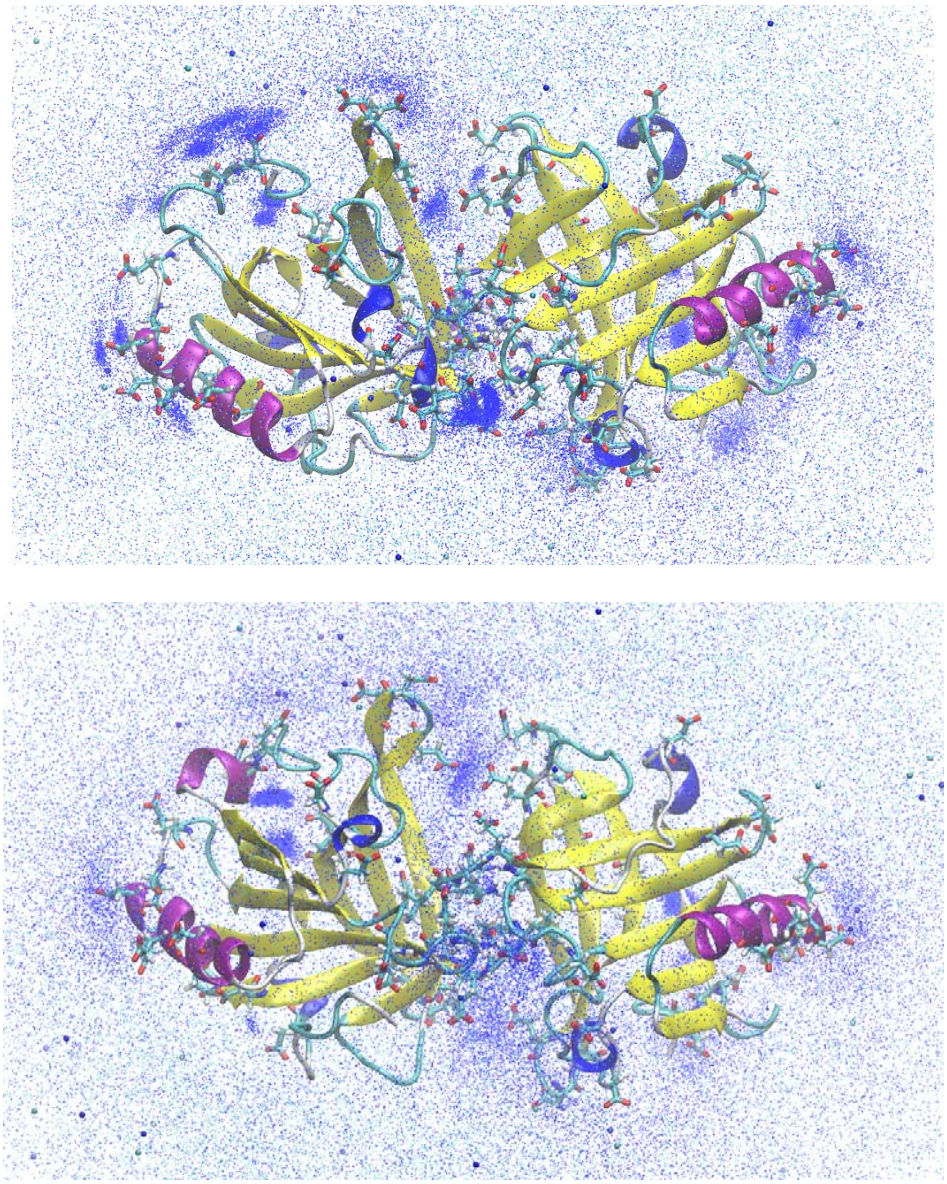

Figure S15. Simulations of dimers based on the monomer structure with loop EF open (2BLG), and the monomers connected via the "loop interface". Protein structure: 209.5 ns, electrolyte: 101.5-209.5 ns, every 5th frame for MCl shown, all frames fitted on minimized X-ray structure, electrolyte concentration 100 mM, Joung/Cheatham ion parameters. Above: NaCl, below: KCl. Sodium and potassium ions are blue, chloride light blue. Figures were created using VMD.[25,26]

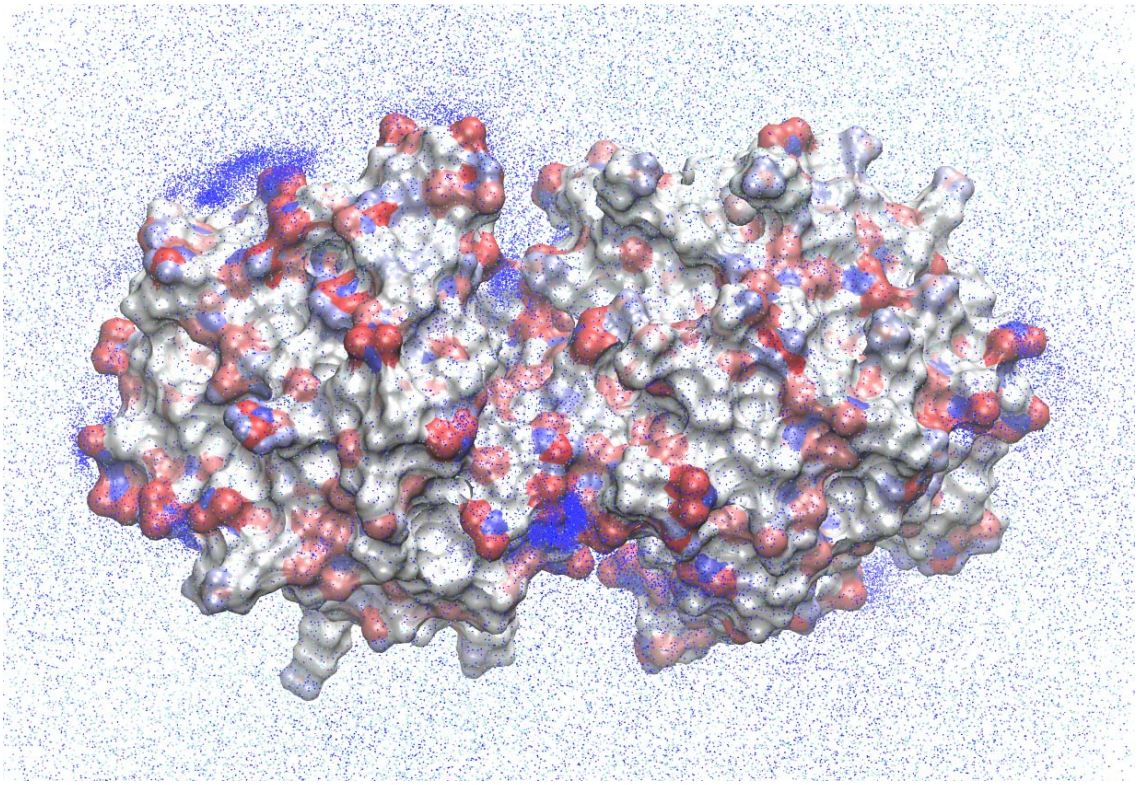

Figure S16. Simulation of dimer based on the monomer structure with loop EF open (2BLG), and the monomers connected via the "loop interface". Protein structure: 209.5 ns (solvent accessible surface colored according to charge, red = negative, blue = positive), electrolyte: 101.5-209.5 ns, every 5th frame for NaCl shown, all frames fitted on minimized X-ray structure, electrolyte concentration 100 mM, Joung/Cheatham ion parameters. Sodium ions are blue, chloride light blue. Figures were created using VMD.[25,26]

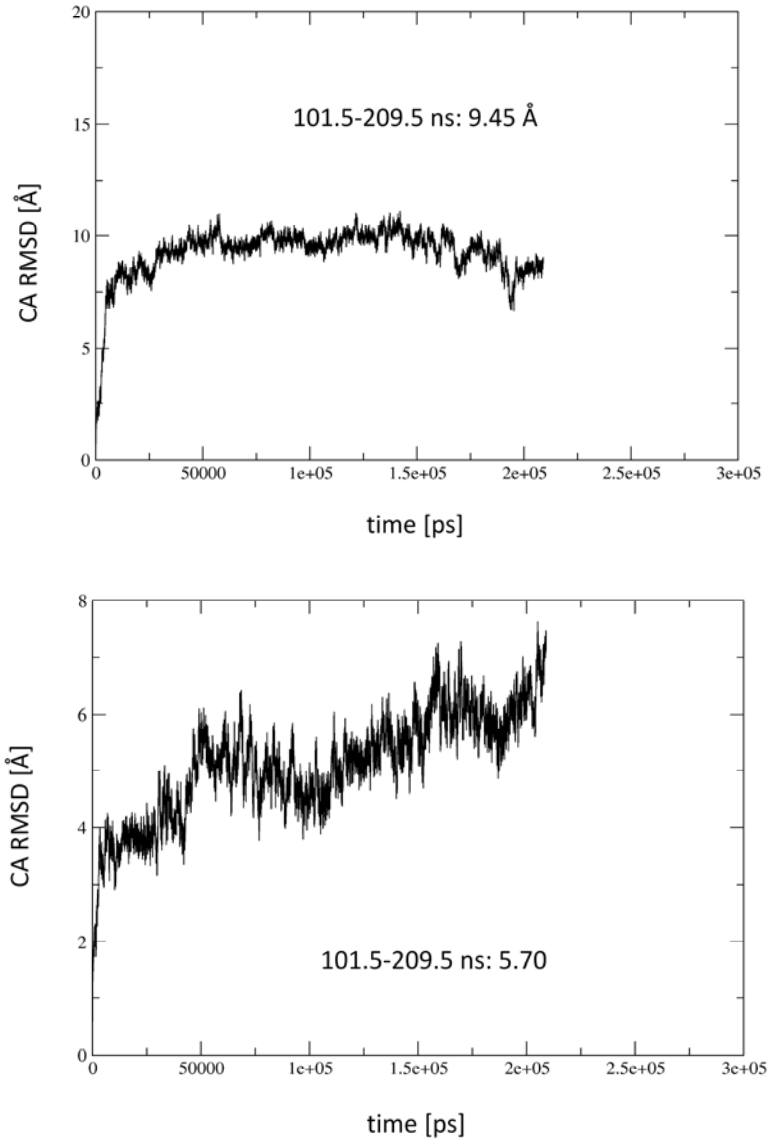

Figure S17. Root mean square deviation (RMSD), calculated for all C_α atoms after fitting each structure on the minimized X-ray structure. Above: simulations with NaCl electrolyte; below: simulations with KCl. Data shown for simulations of dimers based on the monomer structure with loop EF open (2BLG), and the monomers connected via the "loop interface". Analysis interval: 0.5-209.5 ns, additionally mean values are given for 101.5-209.5 ns, all frames were fitted on the minimized X-ray structure before analysis, electrolyte concentration 100 mM, Joung/Cheatham ion parameters were used.

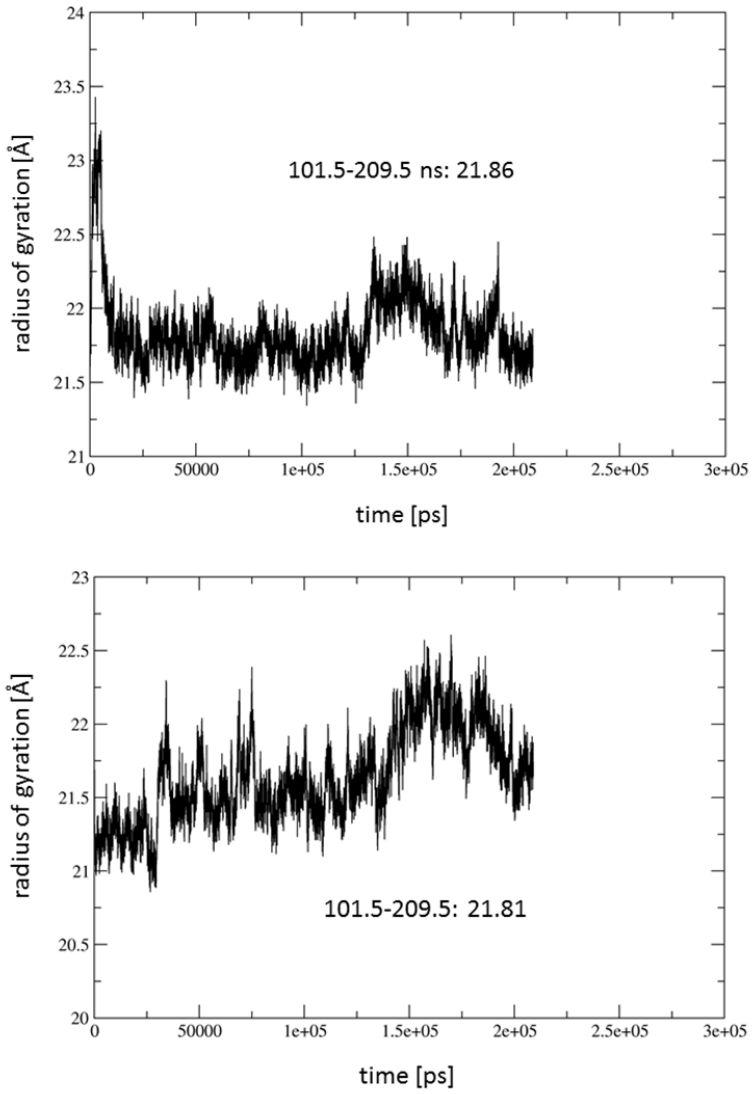

Figure S18. Radius of gyration, calculated for all protein atoms. Above: simulations with NaCl electrolyte; below: simulations with KCl. Data shown for simulations of dimers based on the monomer structure with loop EF open (2BLG), and the monomers connected via the "loop interface". Analysis interval: 0.5-209.5 ns, additionally mean values are given for 101.5-209.5 ns, all frames were fitted on the minimized X-ray structure before analysis, electrolyte concentration 100 mM, Joung/Cheatham ion parameters were used.

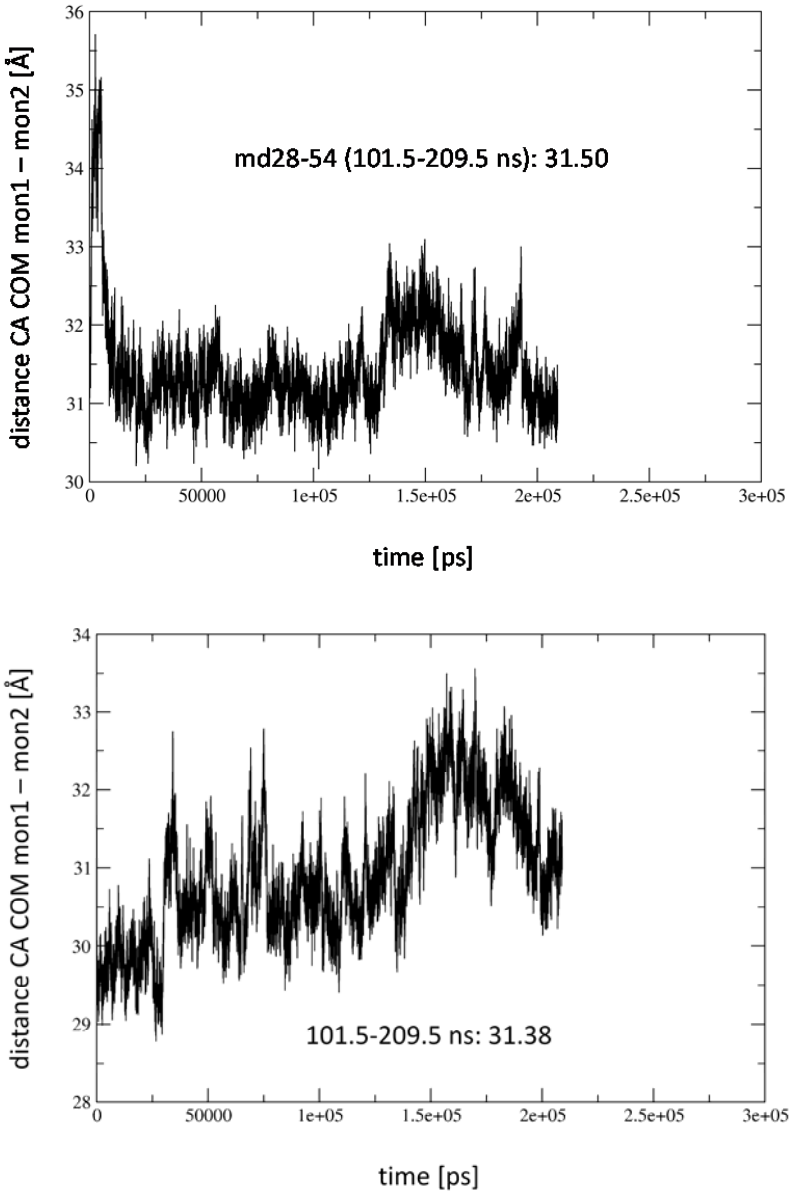

Figure S19. Distance of the centers of mass of all C_α atoms in monomers 1 and 2. Above: simulations with NaCl electrolyte; below: simulations with KCl. Data shown for simulations of dimers based on the monomer structure with loop EF open (2BLG), and the monomers connected via the "loop interface". Analysis interval: 0.5-209.5 ns, additionally mean values are given for 101.5-209.5 ns, all frames were fitted on the minimized X-ray structure before analysis, electrolyte concentration 100 mM, Joung/Cheatham ion parameters were used.

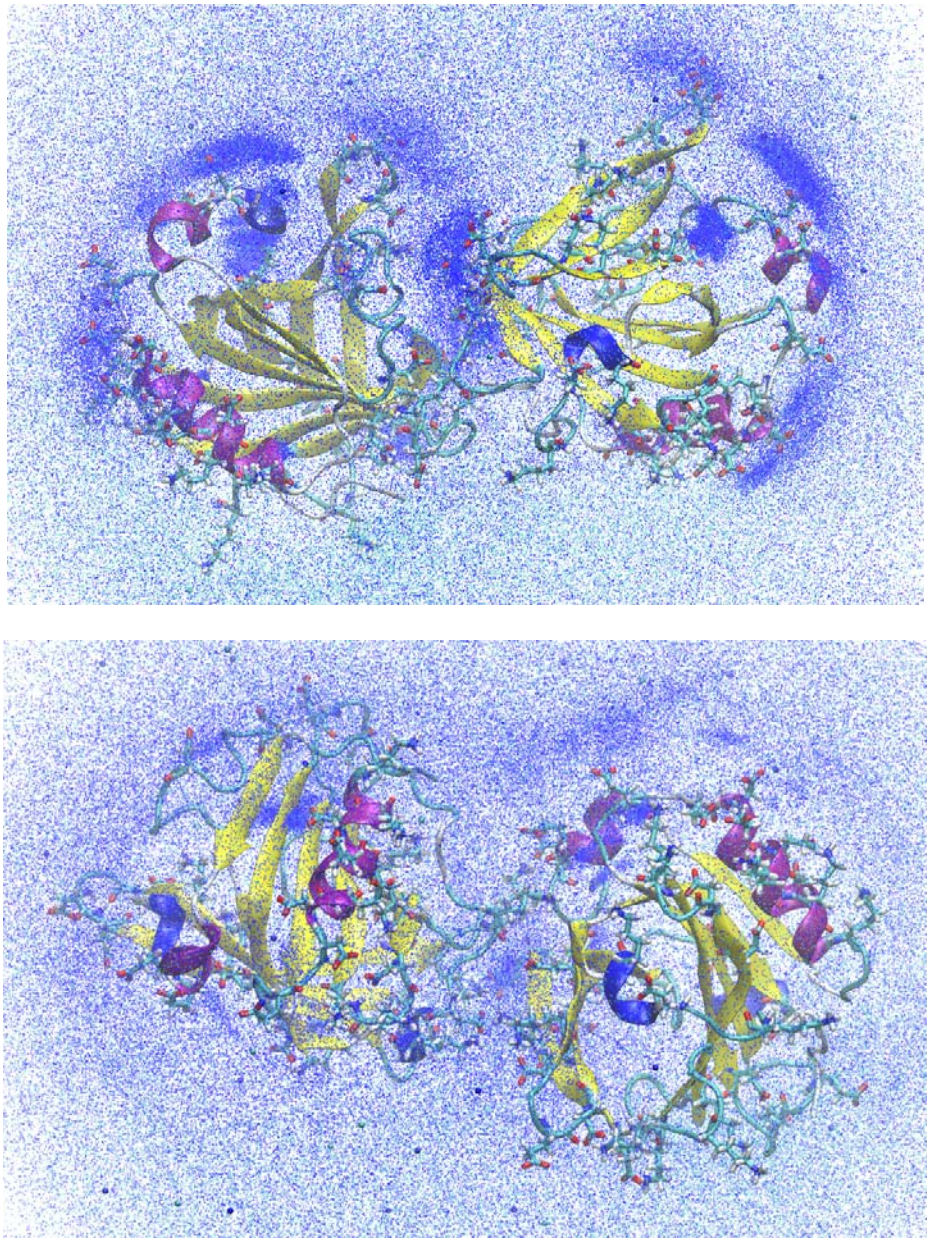

Figure S20. Simulations of dimers based on the monomer structure with loop EF closed (3BLG), and the monomers connected via the "loop Interface". Protein structure: 413.5 ns, electrolyte: 101.5-413.5 ns, every 5th frame for MCl shown, all frames fitted on minimized X-ray structure, electrolyte concentration 100 mM, Joung/Cheatham ion parameters. Above: NaCl, below: KCl. Sodium and potassium ions are blue, chloride light blue. Figures were created using VMD.[25,26]

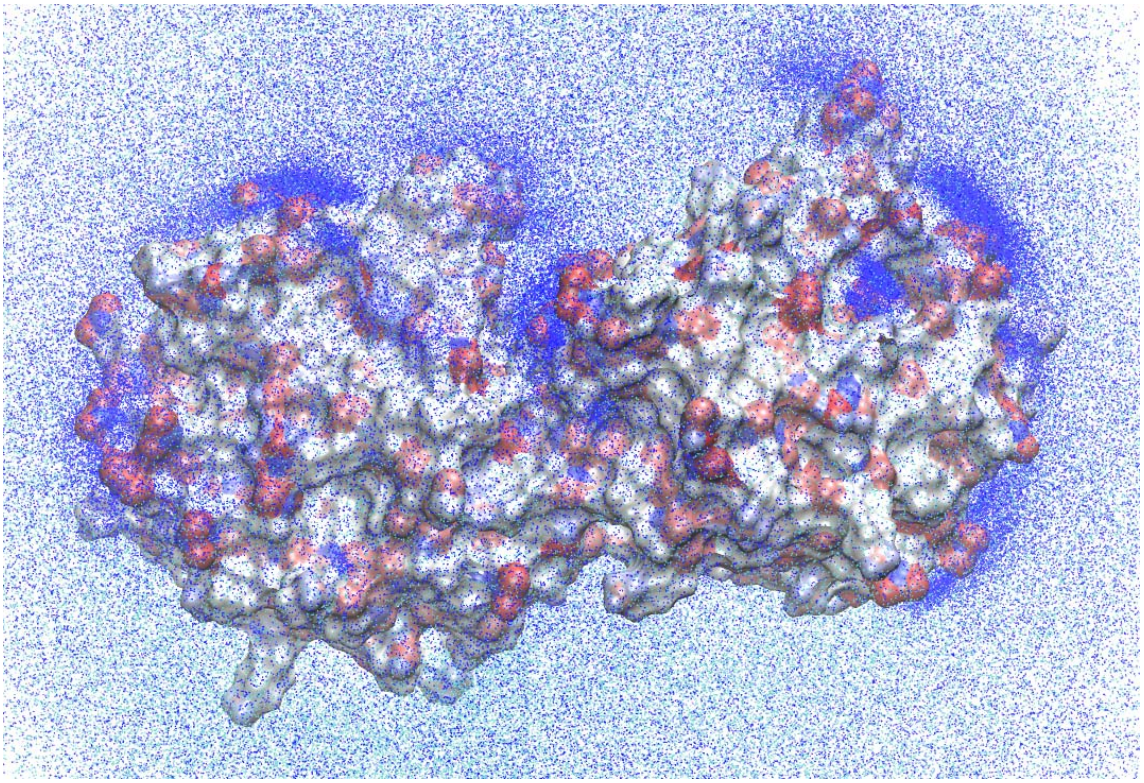

Figure S21. Simulation of dimer based on the monomer structure with loop EF closed (3BLG), and the monomers connected via the "loop Interface". Protein structure: 413.5 ns (solvent accessible surface colored according to charge, red = negative, blue = positive), electrolyte: 101.5-413.5 ns, every 5th frame for NaCl shown, all frames fitted on minimized X-ray structure, electrolyte concentration 100 mM, Joung/Cheatham ion parameters. Sodium ions are blue, chloride light blue. Figures were created using VMD.[25,26]

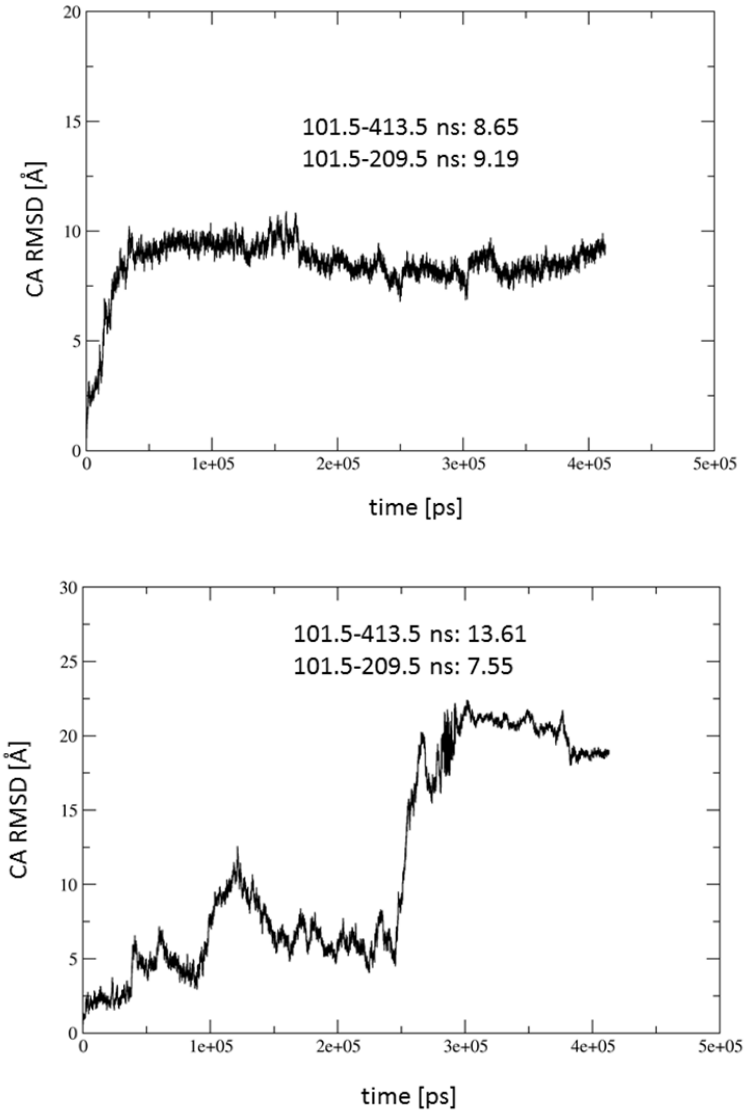

Figure S22. Root mean square deviation (RMSD), calculated for all C_α atoms after fitting each structure on the minimized X-ray structure. Above: simulations with NaCl electrolyte; below: simulations with KCl. Data shown for simulations of dimers based on the monomer structure with loop EF closed (3BLG), and the monomers connected via the "loop interface". Analysis interval: 0.5-413.5 ns, additionally mean values are given for 101.5-413.5 and 101.5-209.5 ns, all frames were fitted on the minimized X-ray structure before analysis, electrolyte concentration 100 mM, Joung/Cheatham ion parameters were used.

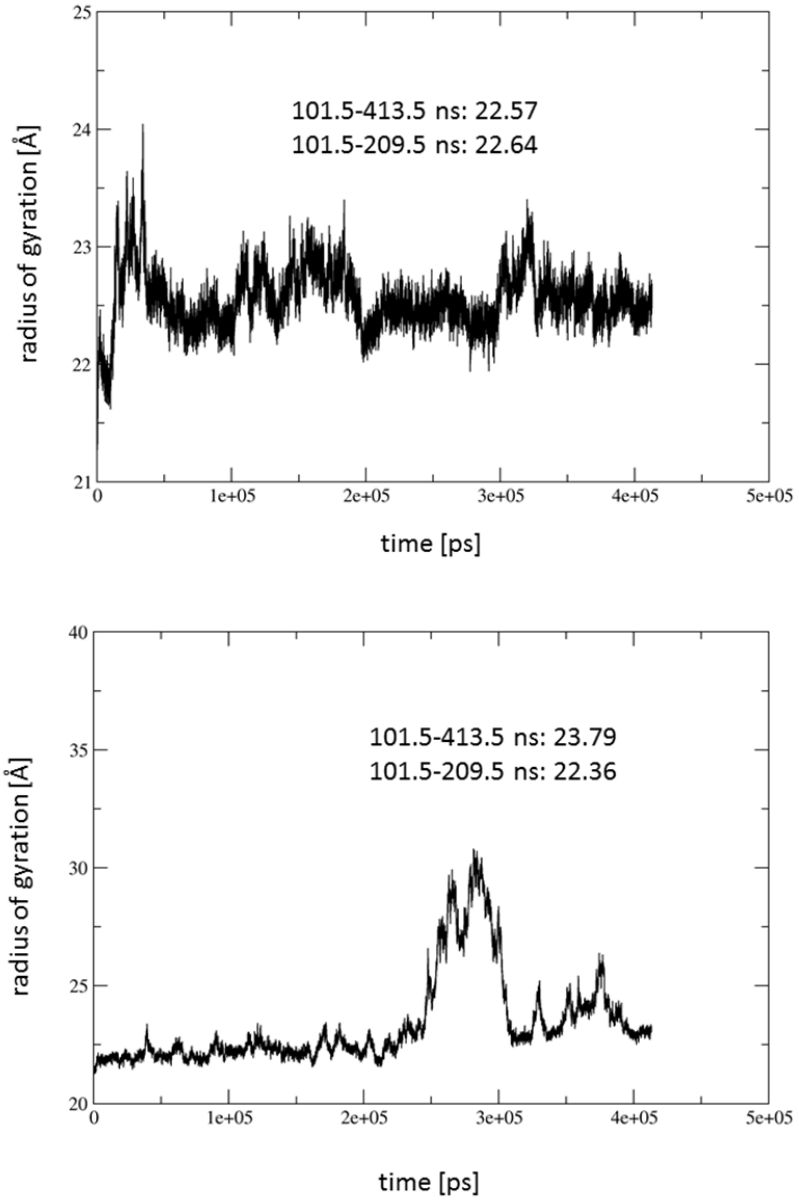

Figure S23. Radius of gyration, calculated for all protein atoms. Above: simulations with NaCl electrolyte; below: simulations with KCl. Data shown for simulations of dimers based on the monomer structure with loop EF closed (3BLG), and the monomers connected via the "loop interface". Analysis interval: 0.5-413.5 ns, additionally mean values are given for 101.5-413.5 and 101.5-209.5 ns, all frames were fitted on the minimized X-ray structure before analysis, electrolyte concentration 100 mM, Joung/Cheatham ion parameters were used.

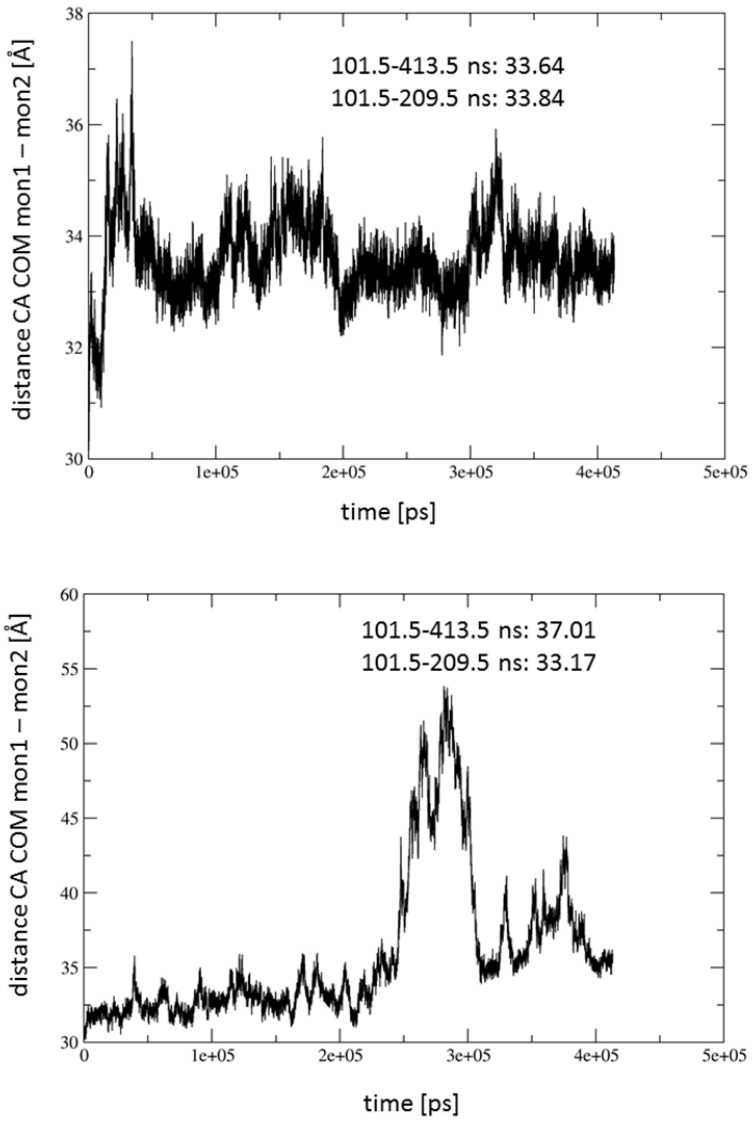

Figure S24. Distance of the centers of mass of all C_α atoms in monomers 1 and 2. Above: simulations with NaCl electrolyte; below: simulations with KCl. Data shown for simulations of dimers based on the monomer structure with loop EF closed (3BLG), and the monomers connected via the "loop interface". Analysis interval: 0.5-413.5 ns, additionally mean values are given for 101.5-413.5 and 101.5-209.5 ns, all frames were fitted on the minimized X-ray structure before analysis, electrolyte concentration 100 mM, Joung/Cheatham ion parameters were used.

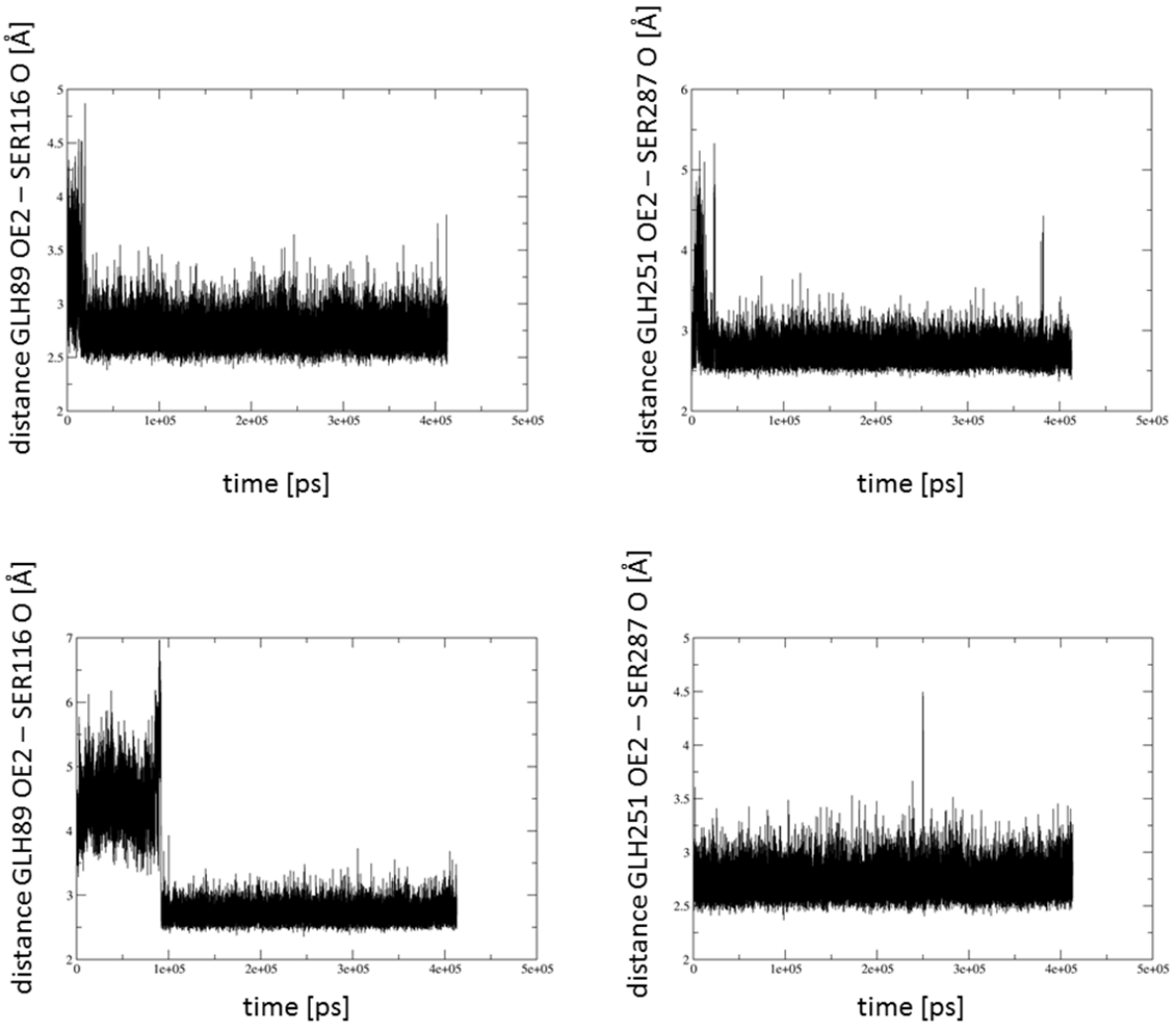

Figure S25. Distance between atoms OE2 of Glh89 and O of Ser116 for monomer 1 (left) and monomer 2 (Glh251 OE2-Ser287 O, right), indicating whether loop EF is closed by formation of a hydrogen bond between these atoms; Above: simulations with NaCl electrolyte; below: simulations with KCl. Data shown for simulations of dimers based on the monomer structure with loop EF closed (3BLG), and the monomers connected via the "loop interface". Analysis interval: 0.5-413.5 ns, all frames were fitted on the minimized X-ray structure before analysis, electrolyte concentration 100 mM, Joung/Cheatham ion parameters were used.

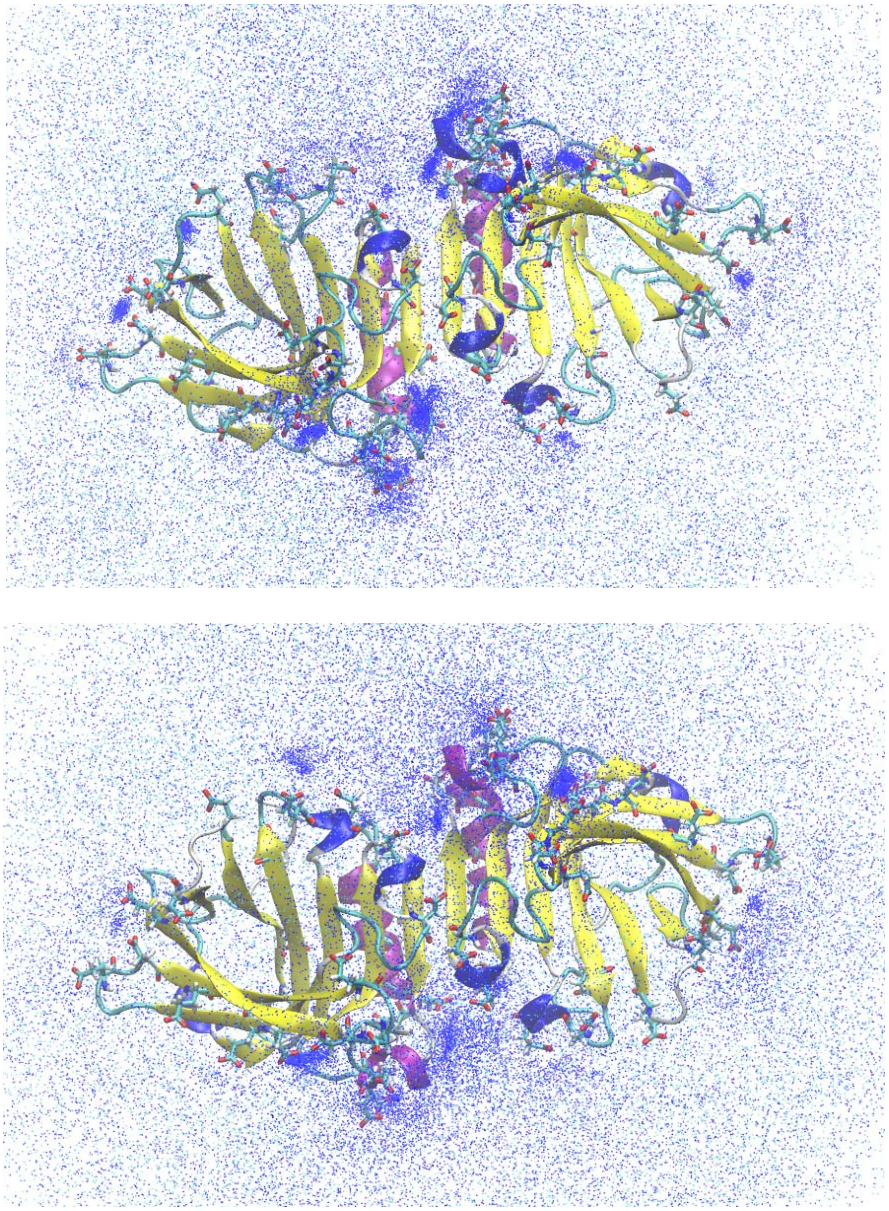

Figure S26. Simulations of dimers based on the monomer structure with loop EF open (2BLG), and the monomers connected via the "dimer Interface". Protein structure: 61.5 ns, electrolyte: 0.5-61.5 ns, every 5th frame for MCl shown, all frames fitted on minimized X-ray structure, electrolyte concentration 100 mM, Joung/Cheatham ion parameters. Above: NaCl, below: KCl. Sodium and potassium ions are blue, chloride light blue. Figures were created using VMD.[25,26]

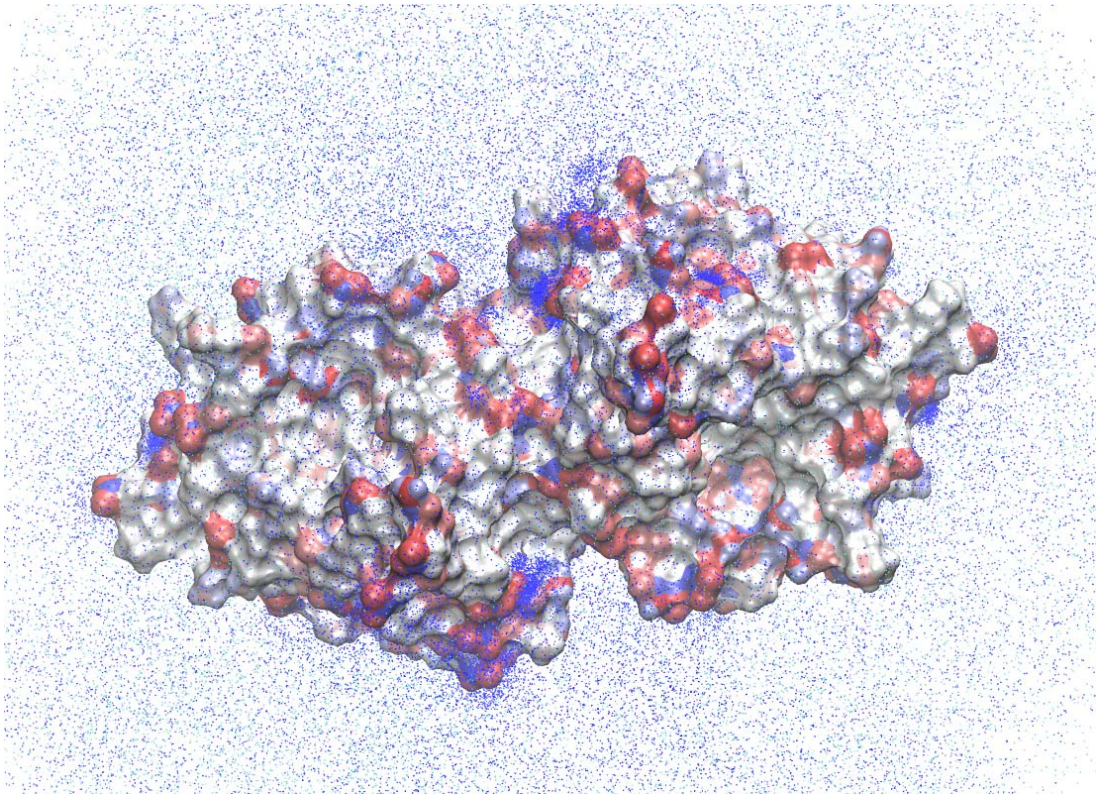

Figure S27. Simulation of dimer based on the monomer structure with loop EF open (2BLG), and the monomers connected via the "dimer Interface". Protein structure: 61.5 ns (solvent accessible surface colored according to charge, red = negative, blue = positive), electrolyte: 0.5-61.5 ns, every 5th frame for NaCl shown, all frames fitted on minimized X-ray structure, electrolyte concentration 100 mM, Joung/Cheatham ion parameters. Sodium ions are blue, chloride light blue. Figures were created using VMD.[25,26]

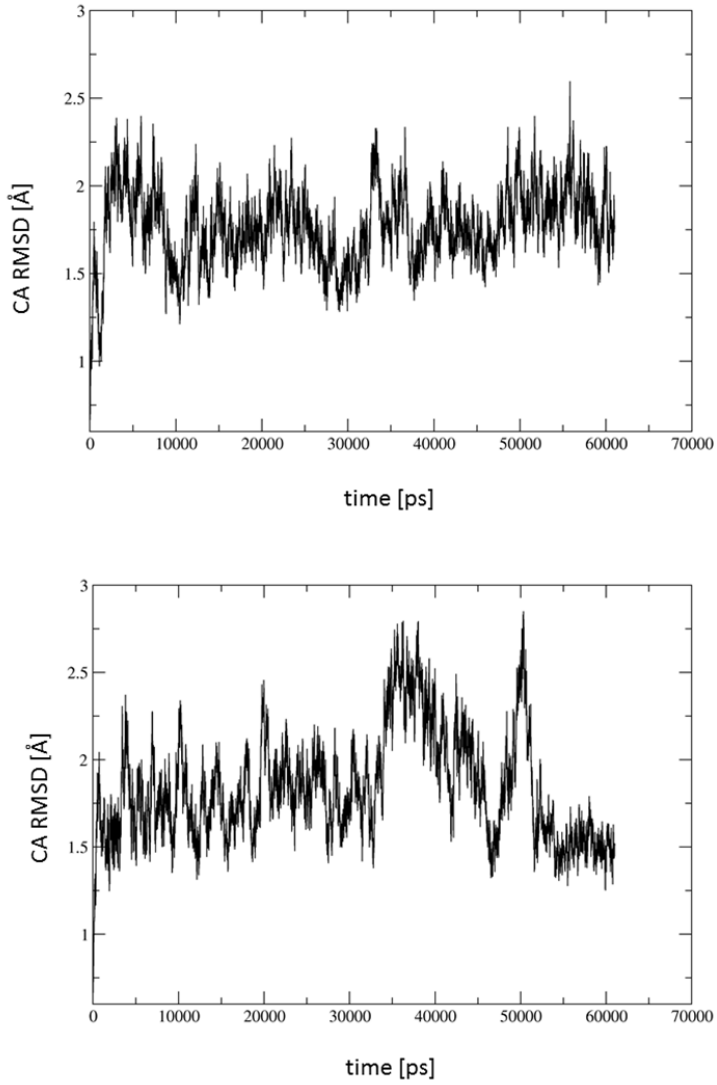

Figure S28. Root mean square deviation (RMSD), calculated for all C_α atoms after fitting each structure on the minimized X-ray structure. Above: simulations with NaCl electrolyte; below: simulations with KCl. Data shown for simulations of dimers based on the monomer structure with loop EF open (2BLG), and the monomers connected via the "dimer interface". Analysis interval: 0.5-209.5 ns, all frames were fitted on the minimized X-ray structure before analysis, electrolyte concentration 100 mM, Joung/Cheatham ion parameters were used.

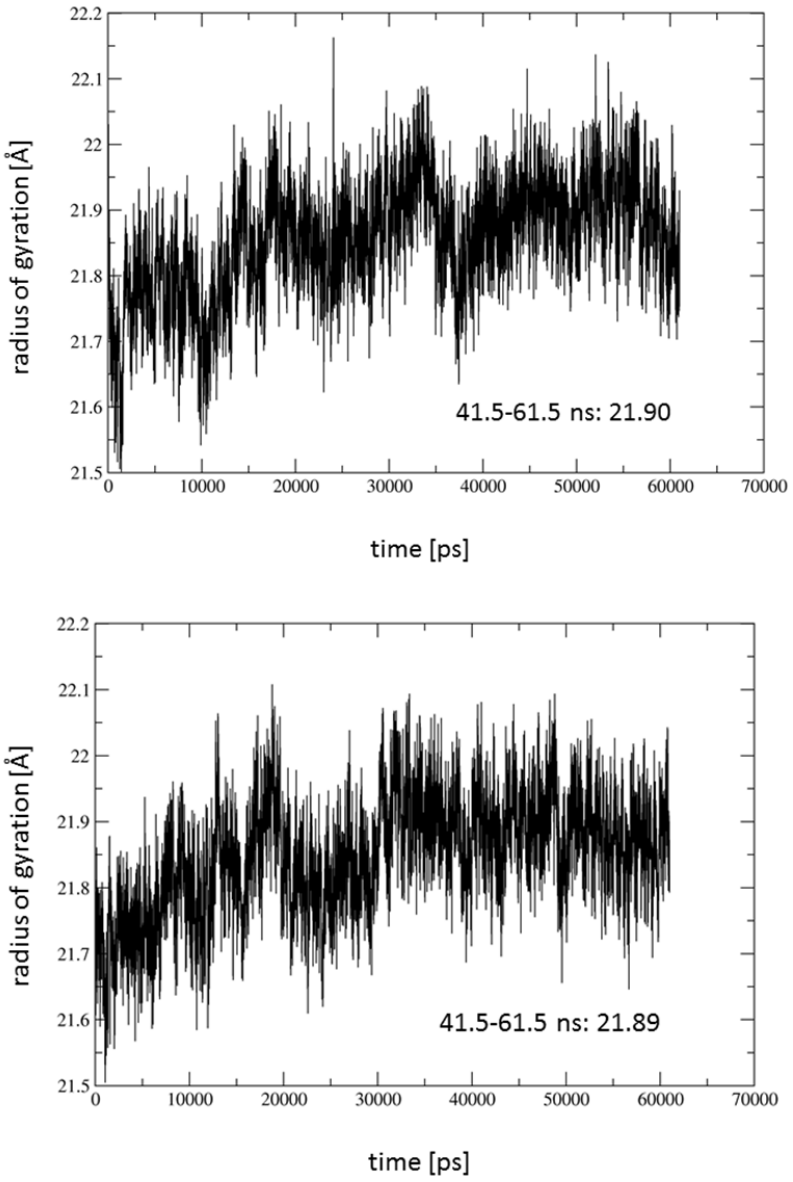

Figure S29. Radius of gyration, calculated for all protein atoms. Above: simulations with NaCl electrolyte; below: simulations with KCl. Data shown for simulations of dimers based on the monomer structure with loop EF open (2BLG), and the monomers connected via the "dimer interface". Analysis interval: 0.5-209.5 ns, all frames were fitted on the minimized X-ray structure before analysis, electrolyte concentration 100 mM, Joung/Cheatham ion parameters were used.

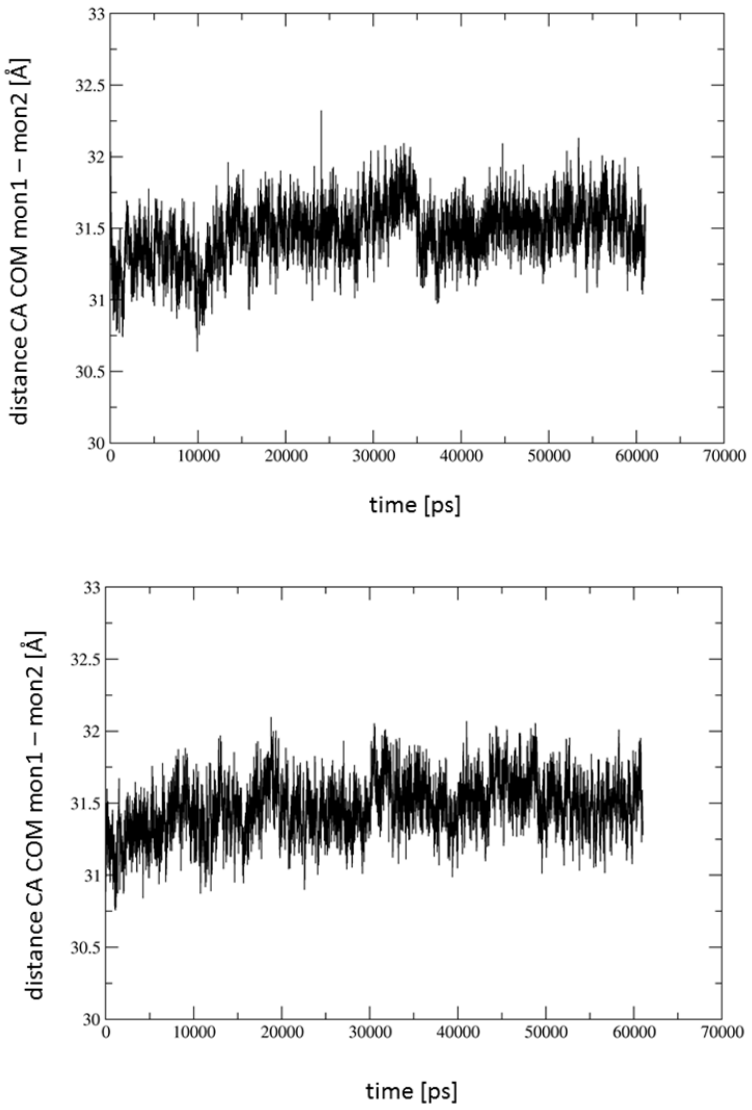

Figure S30. Distance of the centers of mass of all C_α atoms in monomers 1 and 2. Above: simulations with NaCl electrolyte; below: simulations with KCl. Data shown for simulations of dimers based on the monomer structure with loop EF open (2BLG), and the monomers connected via the "dimer interface". Analysis interval: 0.5-209.5 ns, all frames were fitted on the minimized X-ray structure before analysis, electrolyte concentration 100 mM, Joung/Cheatham ion parameters were used.

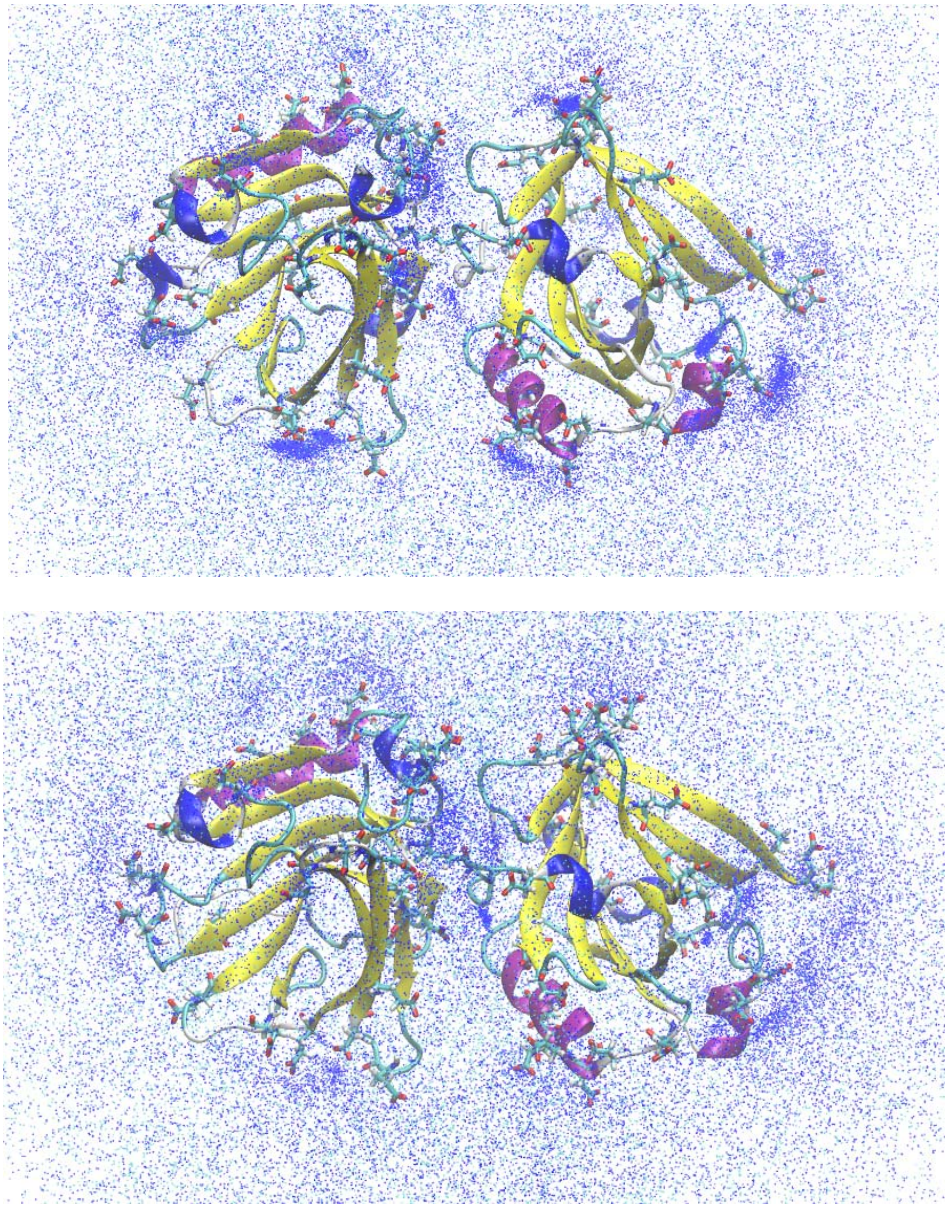

Figure S31. Simulations of dimers based on the monomer structure with loop EF open (2BLG), and the monomers connected via the "lock-and-key interface". Protein structure: 61.5 ns, electrolyte: 0.5-61.5 ns, every 5th frame for MCl shown, all frames fitted on minimized X-ray structure, electrolyte concentration 100 mM, Joung/Cheatham ion parameters. Above: NaCl, below: KCl. Sodium and potassium ions are blue, chloride light blue. Figures were created using VMD.[25,26]

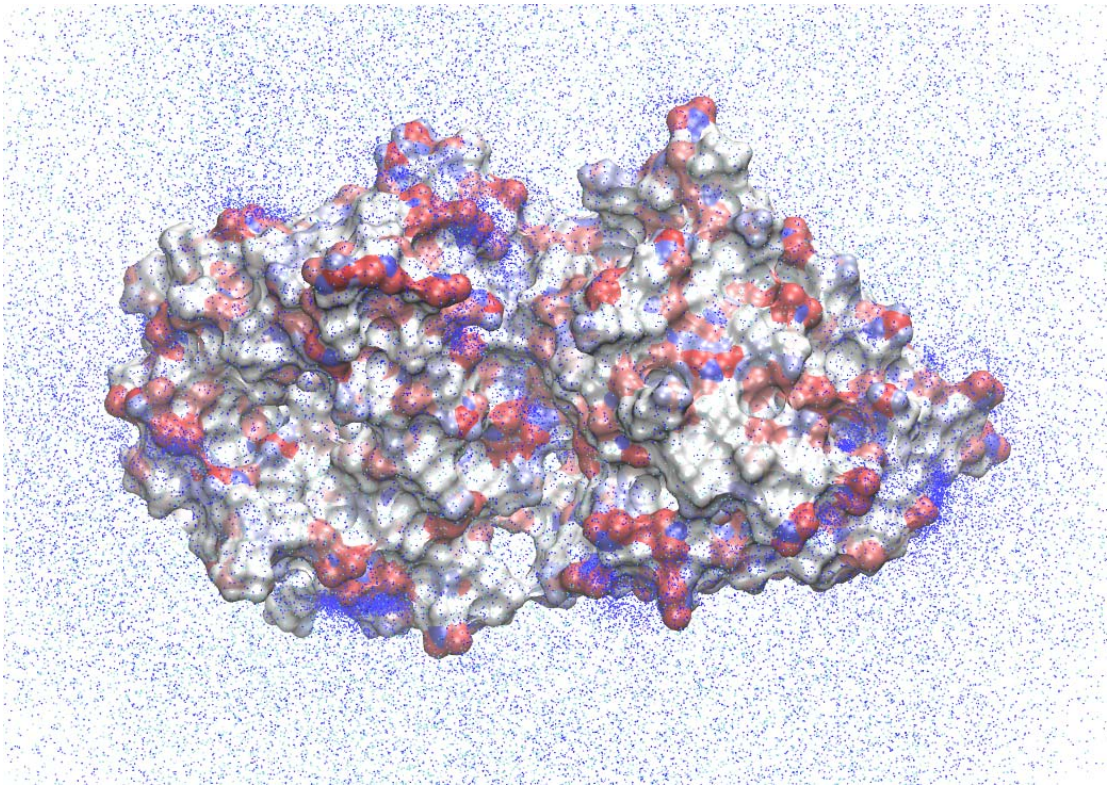

Figure S32. Simulation of dimer based on the monomer structure with loop EF open (2BLG), and the monomers connected via the "lock-and-key interface". Protein structure: 61.5 ns (solvent accessible surface colored according to charge, red = negative, blue = positive), electrolyte: 0.5-61.5 ns, every 5th frame for NaCl shown, all frames fitted on minimized X-ray structure, electrolyte concentration 100 mM, Joung/Cheatham ion parameters. Sodium ions are blue, chloride light blue. Figures were created using VMD.[25,26]

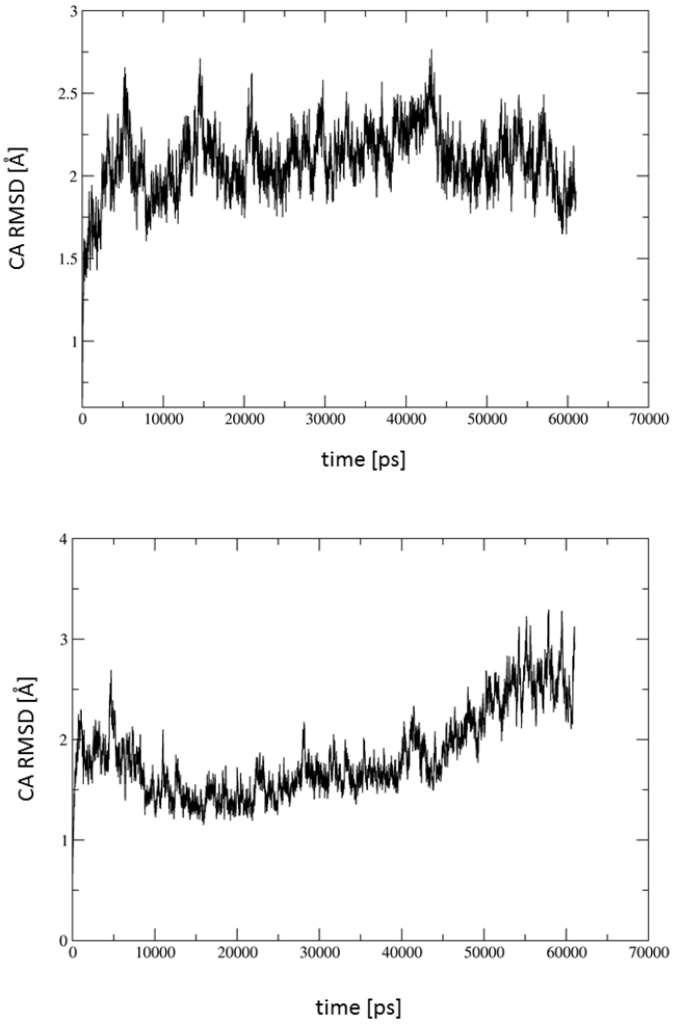

Figure S33. Root mean square deviation (RMSD), calculated for all C_α atoms after fitting each structure on the minimized X-ray structure. Above: simulations with NaCl electrolyte; below: simulations with KCl. Data shown for simulations of dimers based on the monomer structure with loop EF open (2BLG), and the monomers connected via the "lock-and-key interface". Analysis interval: 0.5-209.5 ns, all frames were fitted on the minimized X-ray structure before analysis, electrolyte concentration 100 mM, Joung/Cheatham ion parameters were used.

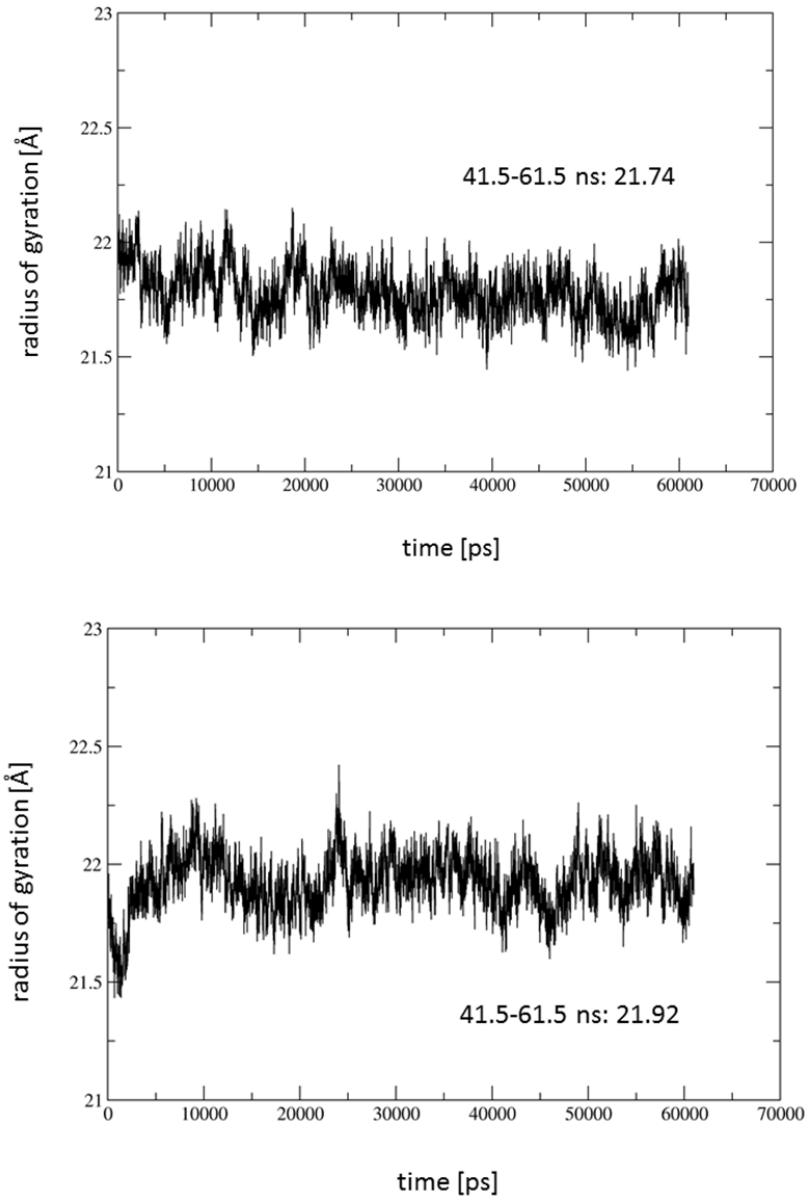

Figure S34. Radius of gyration, calculated for all protein atoms. Above: simulations with NaCl electrolyte; below: simulations with KCl. Data shown for simulations of dimers based on the monomer structure with loop EF open (2BLG), and the monomers connected via the "lock-and-key interface". Analysis interval: 0.5-209.5 ns, all frames were fitted on the minimized X-ray structure before analysis, electrolyte concentration 100 mM, Joung/Cheatham ion parameters were used.

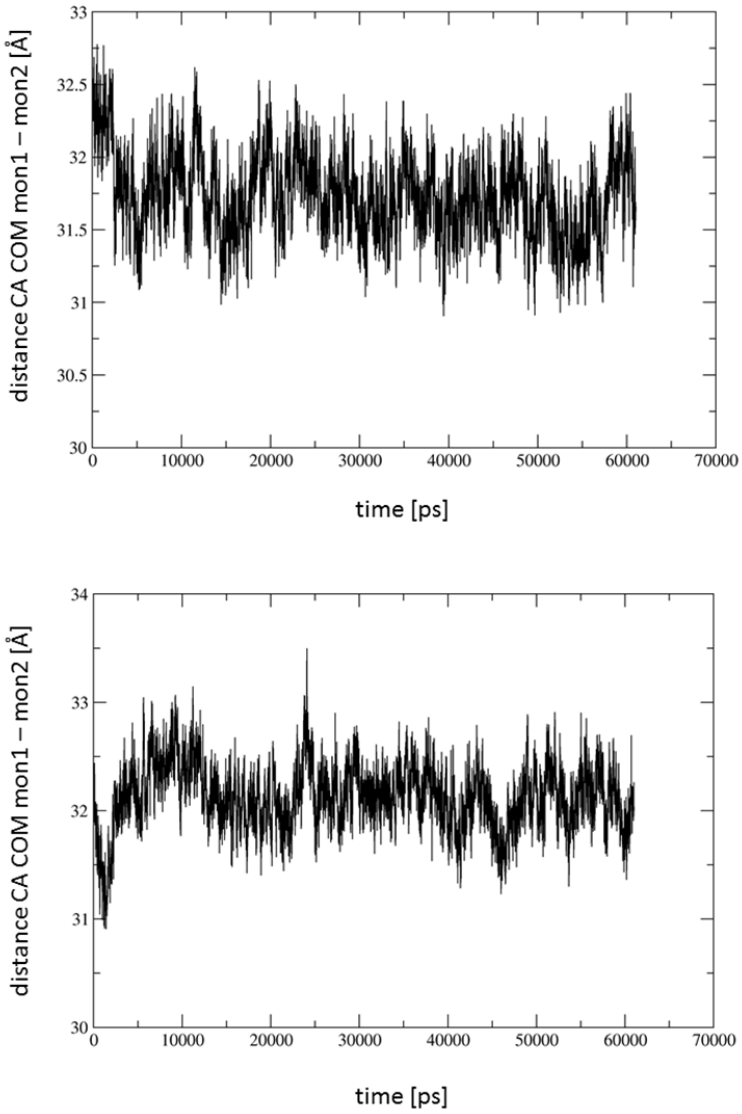

Figure S35. Distance of the centers of mass of all C_α atoms in monomers 1 and 2. Above: simulations with NaCl electrolyte; below: simulations with KCl. Data shown for simulations of dimers based on the monomer structure with loop EF open (2BLG), and the monomers connected via the "lock-and-key interface". Analysis interval: 0.5-209.5 ns, all frames were fitted on the minimized X-ray structure before analysis, electrolyte concentration 100 mM, Joung/Cheatham ion parameters were used.

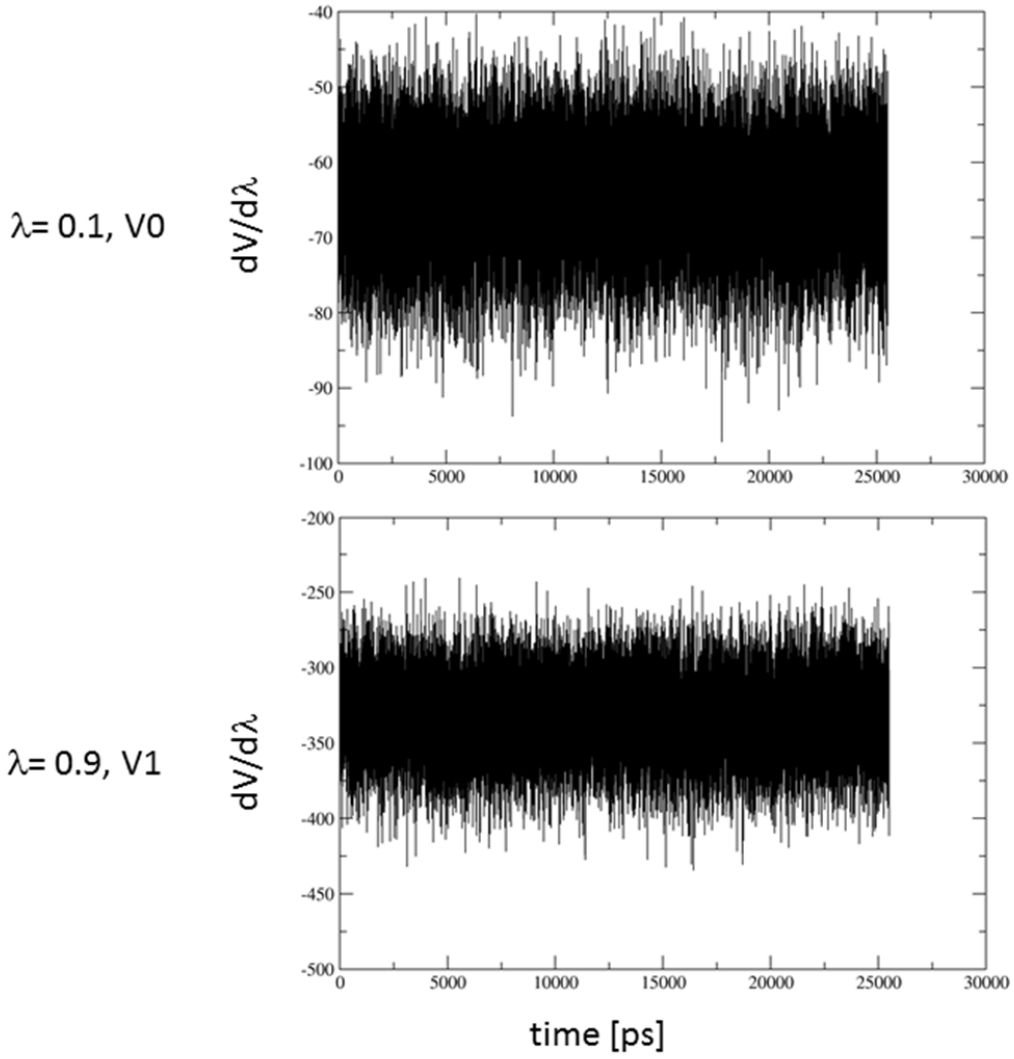

Figure S36. Gradients dV/dλ vs. simulation time, data given for λ = 0.1 ("K^+-like") and λ = 0.9 ("Na^+-like"). "Bound" simulation (i.e., ions, protein and water present). Monomer with protonated Glh74.

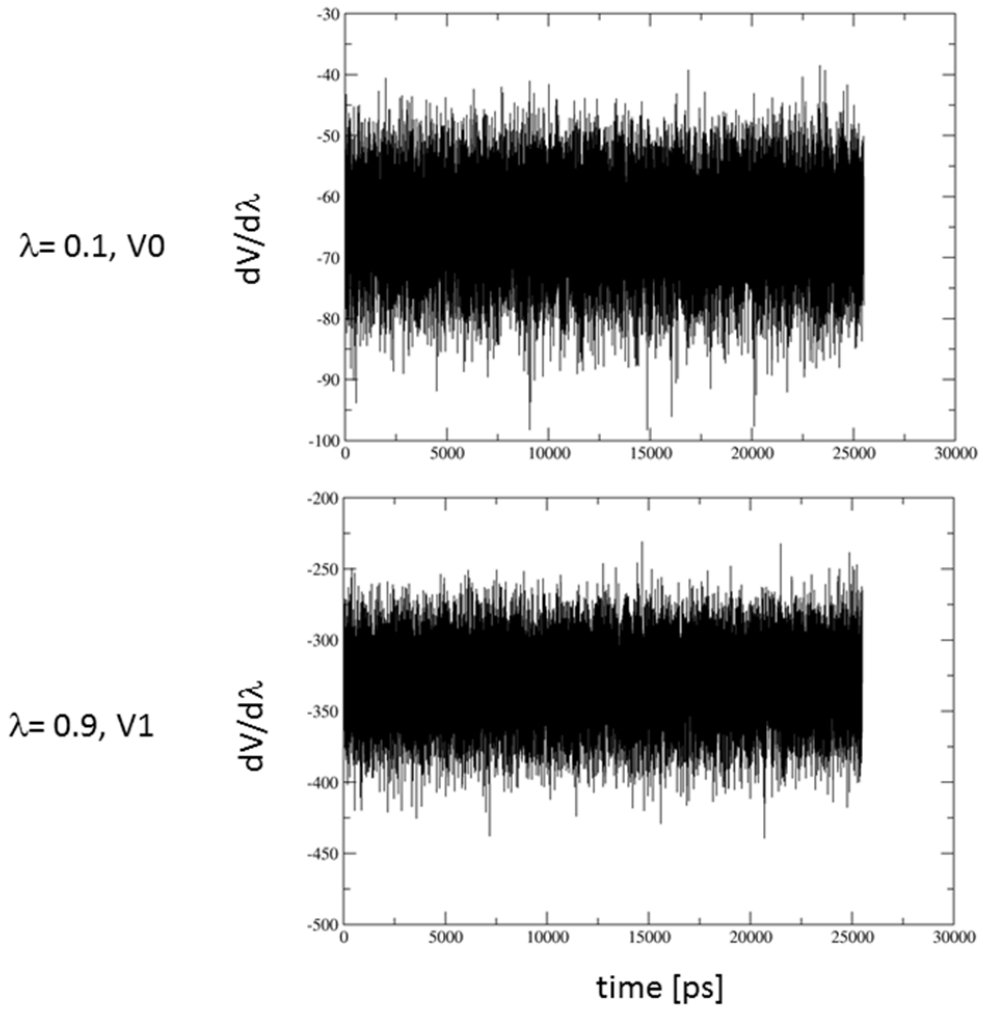

Figure S37. Gradients dV/dλ vs. simulation time, data given for λ = 0.1 ("K^+-like") and λ = 0.9 ("Na^+-like"). "Free" simulation (i.e., ions, and water present). Number of ions and water molecules as in monomer simulation.

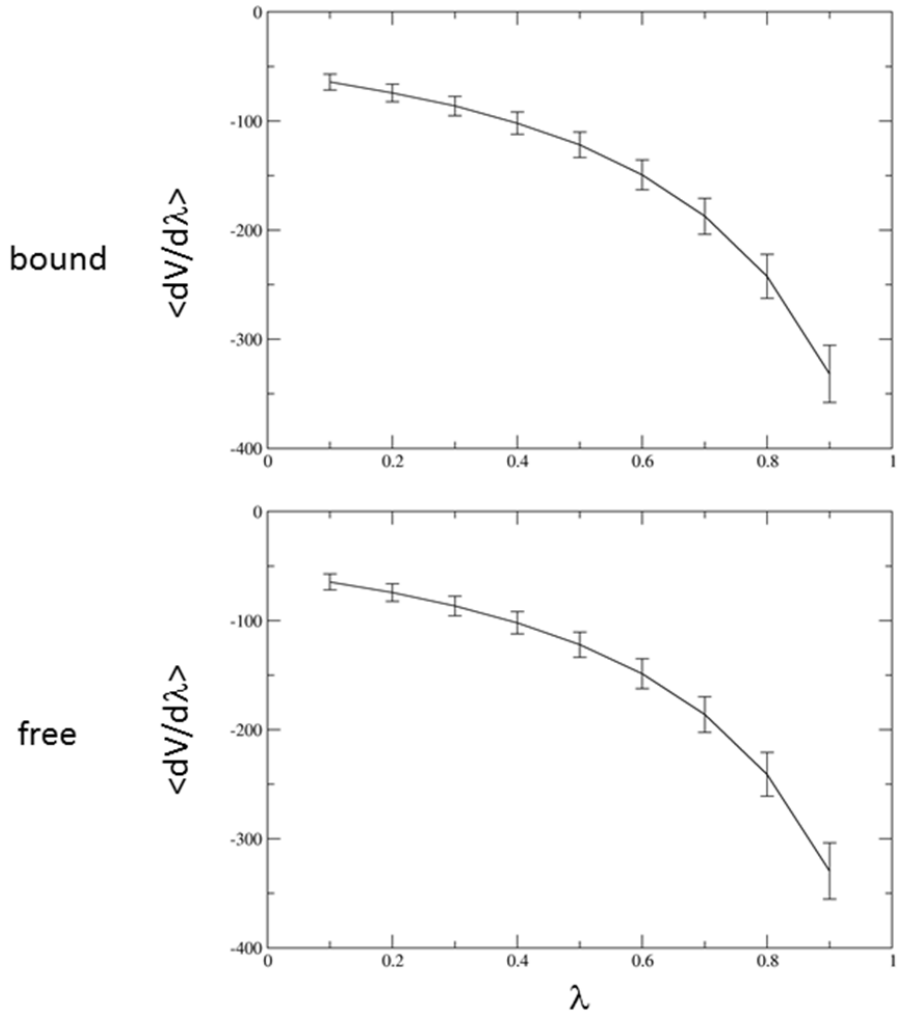

Figure S38. Ensemble averages of gradients <dV/dλ> vs. λ, data given exemplary for 23.5-25.5 ns. Monomer simulation with protonated Glh74.

Table S2. Integrated perturbation free energies, given for partial trajectories (2 ns each). SD: standard deviation, SE: standard error. "Bound" simulation (i.e., ions, protein and water present). Monomer with protonated Glh74.

MD	time [ns]	ΔG_{pert} [kcal.mol^{-1}]
3	3.5	-159.31
4	5.5	-159.87
5	7.5	-159.86
6	9.5	-159.54
7	11.5	-159.66
8	13.5	-159.45
9	15.5	-159.26
10	17.5	-159.94
11	19.5	-159.96
12	21.5	-159.64
13	23.5	-159.17
14	25.5	-159.74
md5-14	mean	-159.62
	SD	0.26
	SE	0.08

Table S3. Integrated perturbation free energies, given for partial trajectories (2 ns each). SD: standard deviation, SE: standard error. "Free" simulation (i.e., ions, and water present). Number of ions and water molecules as in monomer simulation.

MD	time [ns]	ΔG_{pert} [kcal.mol^{-1}]
3	3.5	-159.06
4	5.5	-159.19
5	7.5	-159.22
6	9.5	-159.05
7	11.5	-159.06
8	13.5	-159.02
9	15.5	-159.12
10	17.5	-159.14
11	19.5	-159.21
12	21.5	-159.18
13	23.5	-159.09
14	25.5	-159.14
md5-14	mean	-159.12
	SD	0.06
	SE	0.02

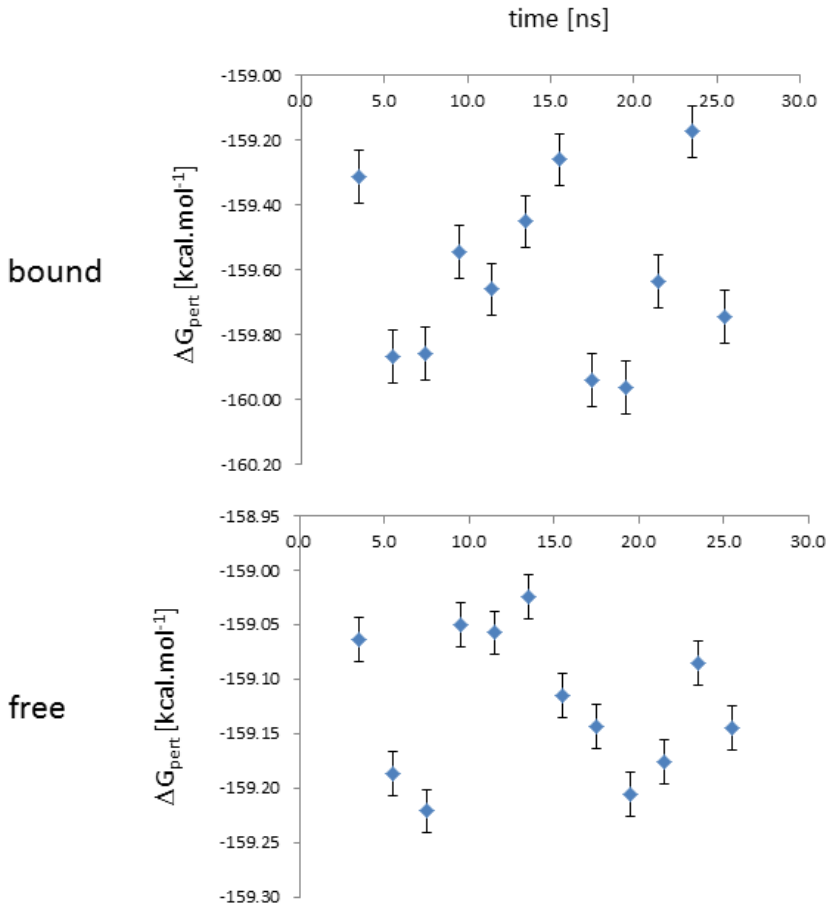

Figure S39. Integrated perturbation free energies, given for partial trajectories (2 ns each) vs. simulation time. Error bars are standard errors from batch averaging. Monomer with protonated Glh74.

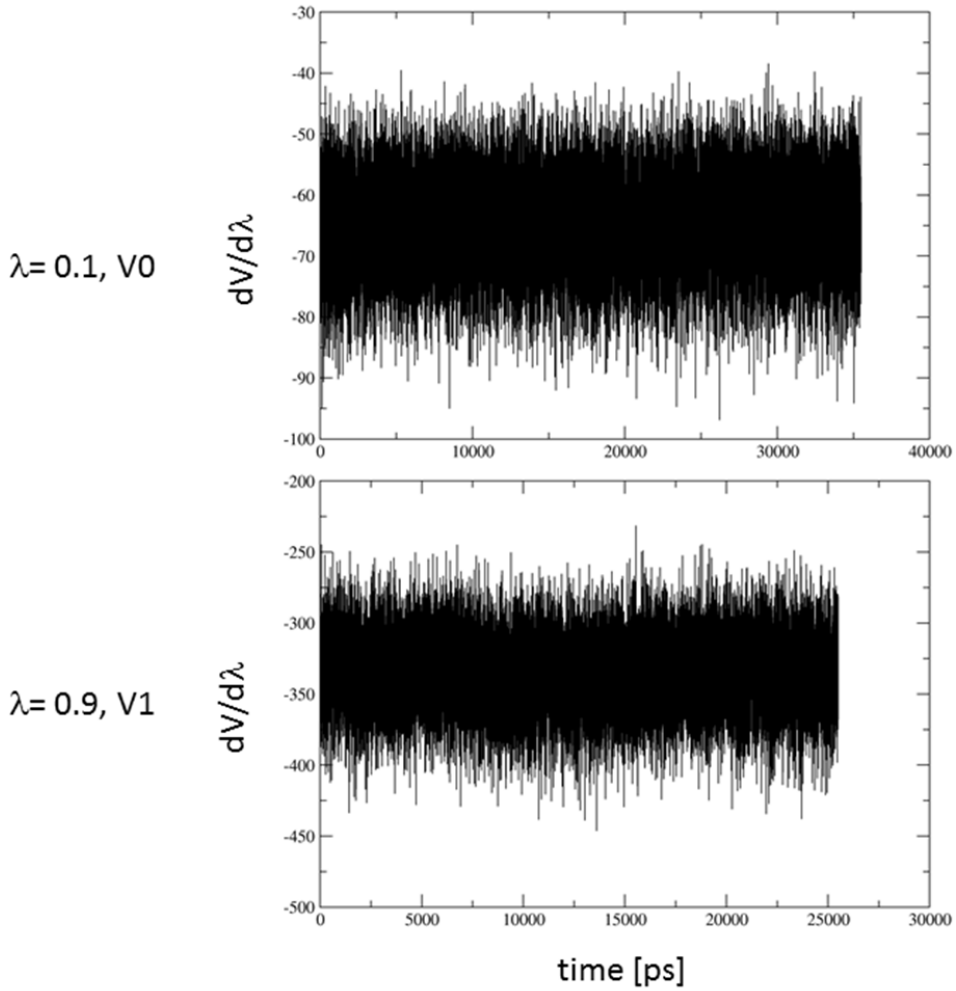

Figure S40. Gradients dV/dλ vs. simulation time, data given for λ = 0.1 ("K^+-like") and λ = 0.9 ("Na^+-like"). "Bound" simulation (i.e., ions, protein and water present). Monomer with alternative protonation state (Glh131 instead of Glh74).

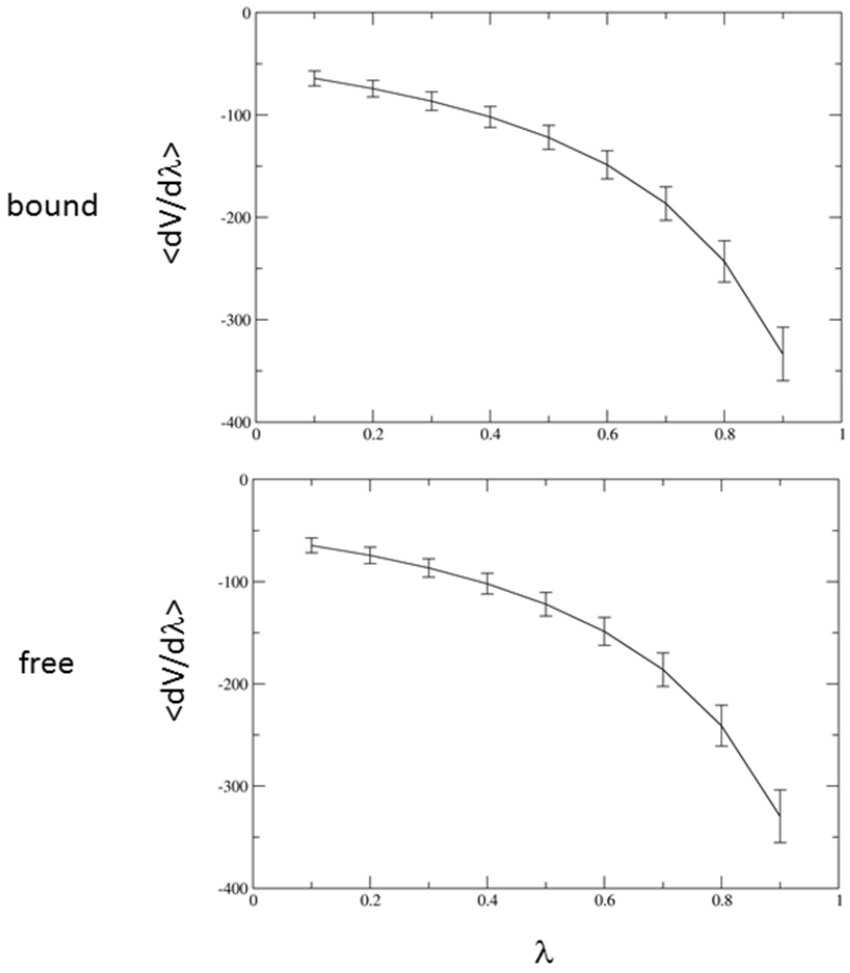

Figure S41. Ensemble averages of gradients <dV/dλ> vs. λ, data given exemplary for 33.5-35.5 ns (bound) and 23.5-25.5 ns (free). Monomer with alternative protonation state (Glh131 instead of Glh74).

Table S4. Integrated perturbation free energies, given for partial trajectories (2 ns each). SD: standard deviation, SE: standard error. "Bound" simulation (i.e., ions, protein and water present). Monomer with alternative protonation state (Glh131 instead of Glh74).

MD	time [ns]	ΔG_{pert} [kcal.mol^{-1}]
3	3.5	-159.673385
4	5.5	-159.225675
5	7.5	-159.530955
6	9.5	-160.46284
7	11.5	-160.58615
8	13.5	-161.013155
9	15.5	-160.62869
10	17.5	-160.049535
11	19.5	-159.94907
12	21.5	-160.00807
13	23.5	-160.103585
14	25.5	-160.14084
15	27.5	-160.13263
16	29.5	-160.476255
17	31.5	-160.075305
18	33.5	-160.3271
19	35.5	-159.97054
md10-19	mean	-160.12
	SD	0.16
	SE	0.05

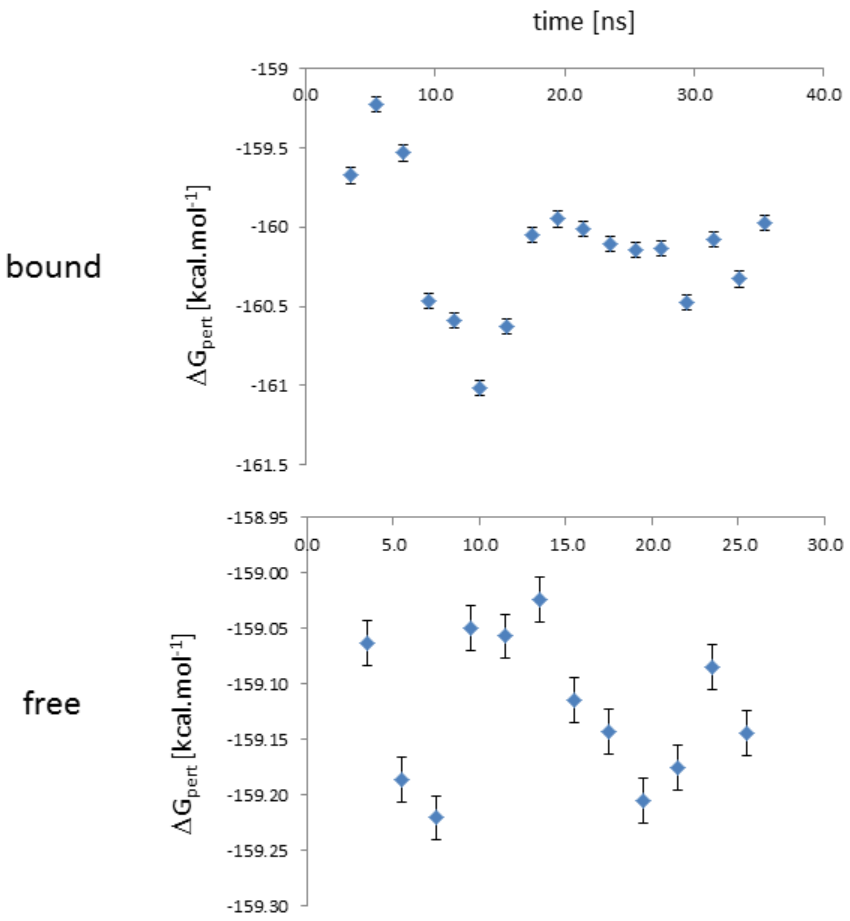

Figure S42. Integrated perturbation free energies, given for partial trajectories (2 ns each) vs. simulation time. Error bars are standard errors from batch averaging. Monomer with alternative protonation state (Glh131 instead of Glh74).

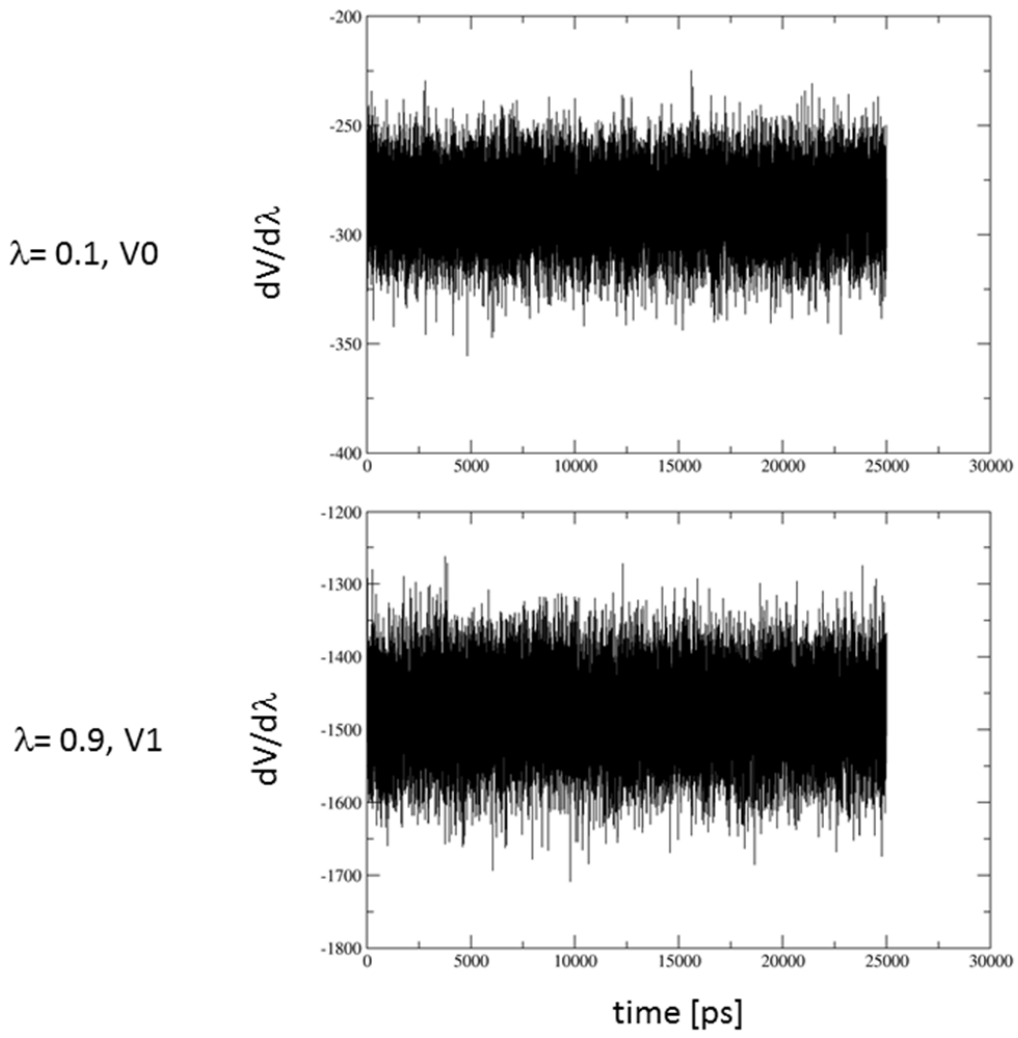

Figure S43. Gradients dV/dλ vs. simulation time, data given for λ = 0.1 ("K^+-like") and λ = 0.9 ("Na^+-like"). "Bound" simulation (i.e., ions, protein and water present) of dimer.

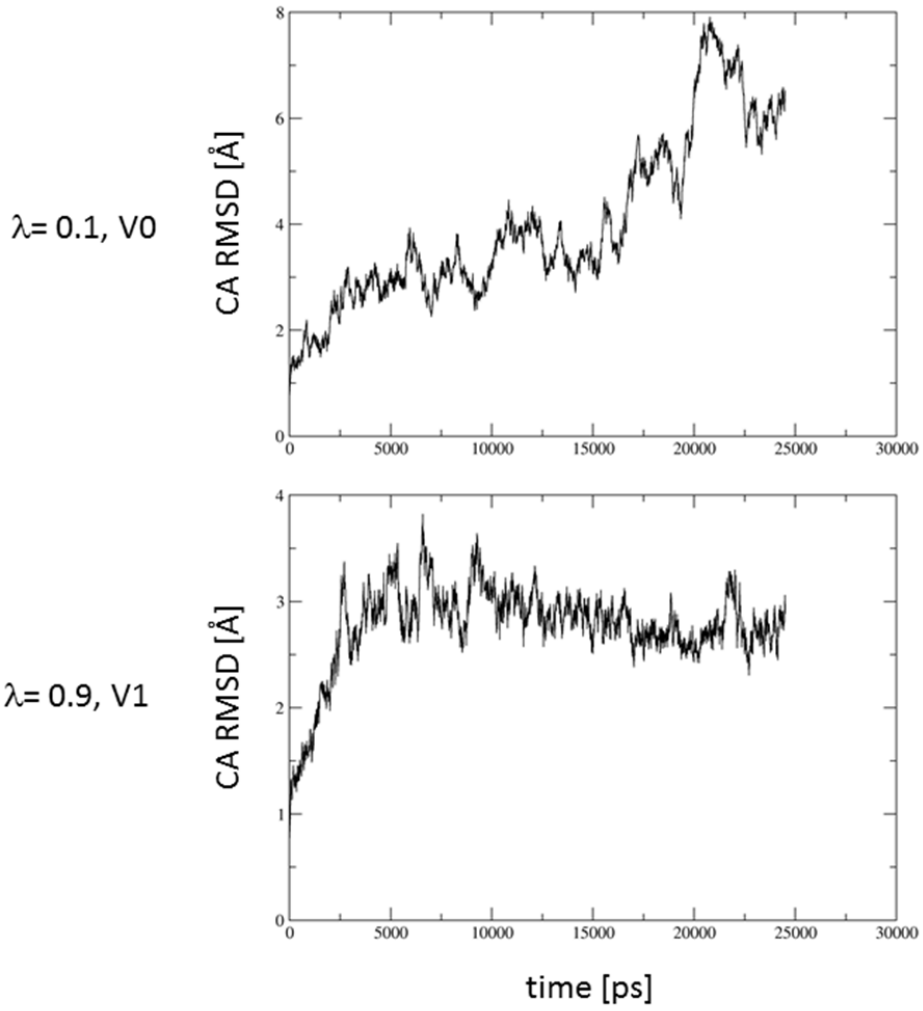

Figure S44. Root mean square deviation (RMSD), calculated for all C_α atoms after fitting each structure on the minimized X-ray structure, vs. simulation time; data given for λ = 0.1 ("K^+-like") and λ = 0.9 ("Na^+-like"). "Bound" simulation (i.e., ions, protein and water present) of dimer.

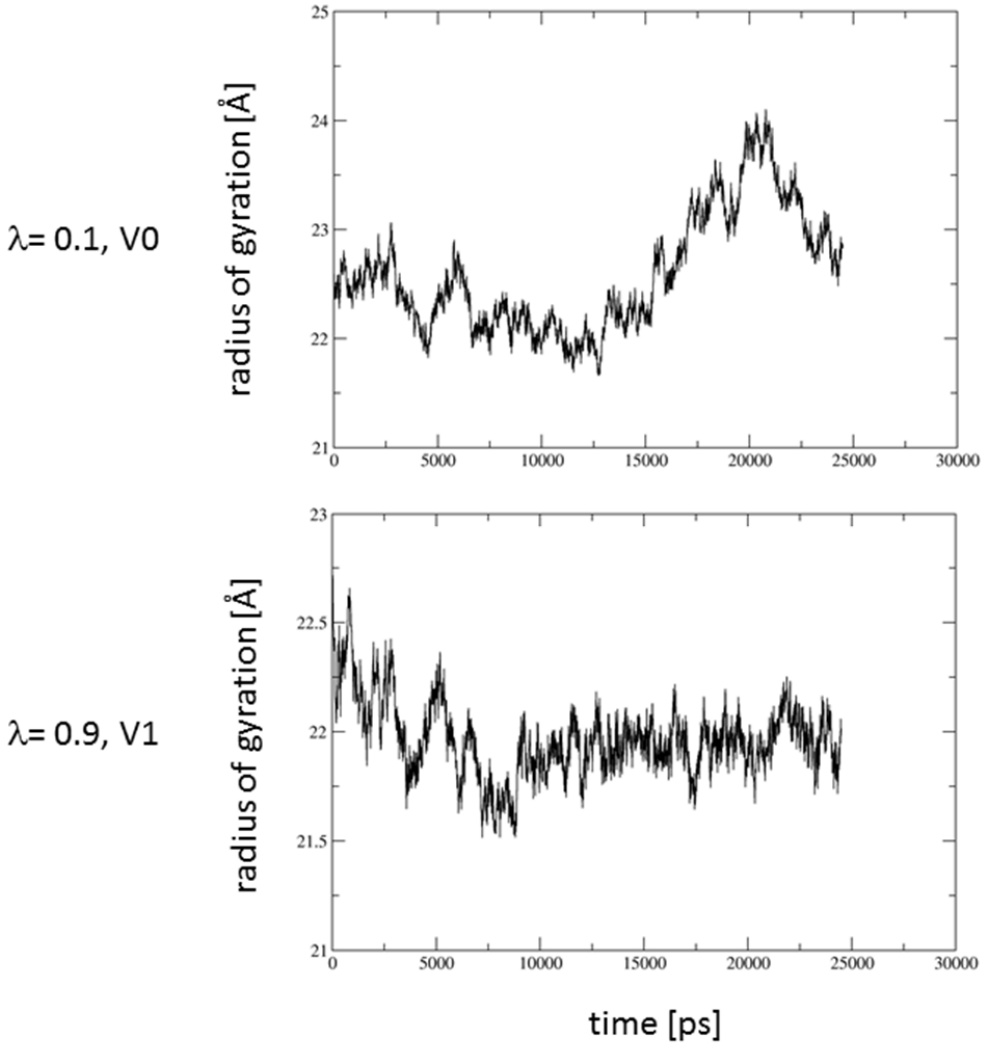

Figure S45. Radius of gyration, calculated for all protein atoms vs. simulation time; data given for $\lambda = 0.1$ ("K^+-like") and $\lambda = 0.9$ ("Na^+-like"). "Bound" simulation (i.e., ions, protein and water present) of dimer.

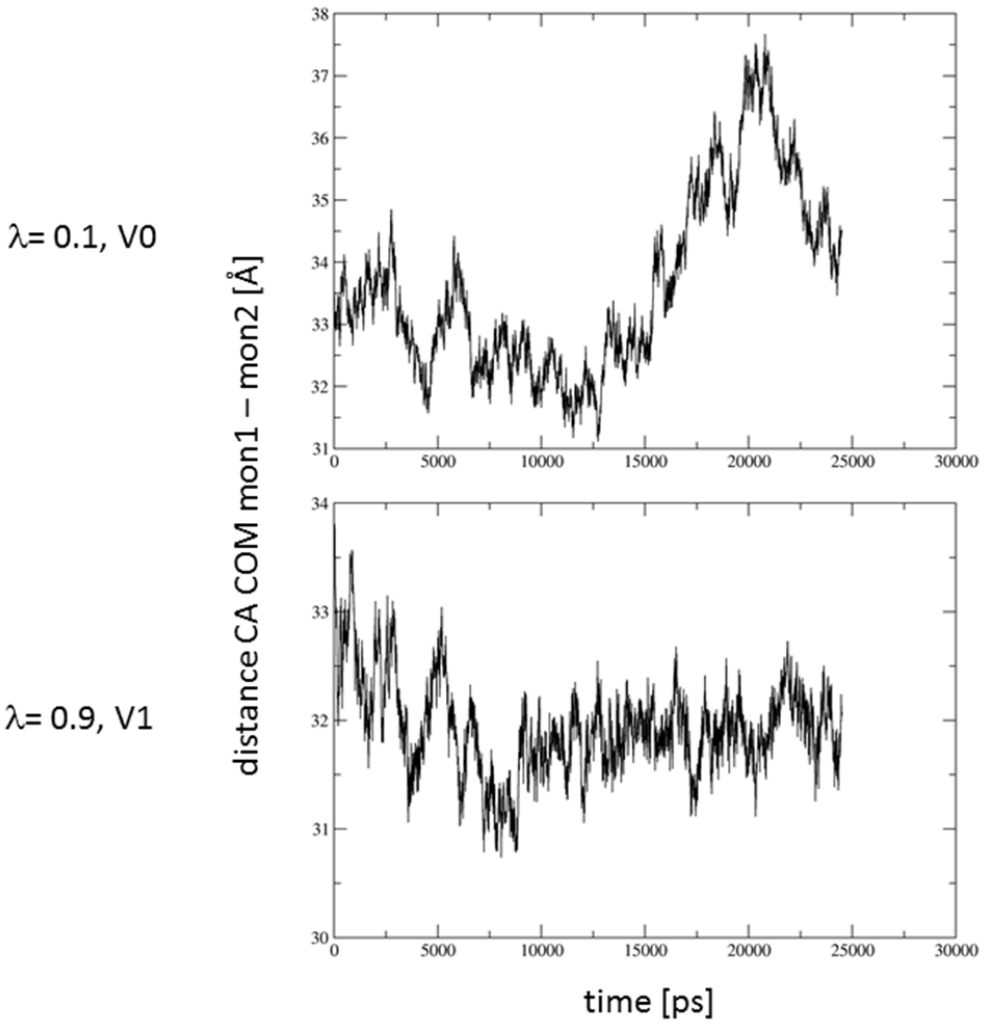

Figure S46. Distance of the centers of mass of all C_α atoms in monomers 1 and 2. vs. simulation time; data given for $\lambda = 0.1$ ("K^+-like") and $\lambda = 0.9$ ("Na^+-like"). "Bound" simulation (i.e., ions, protein and water present) of dimer.

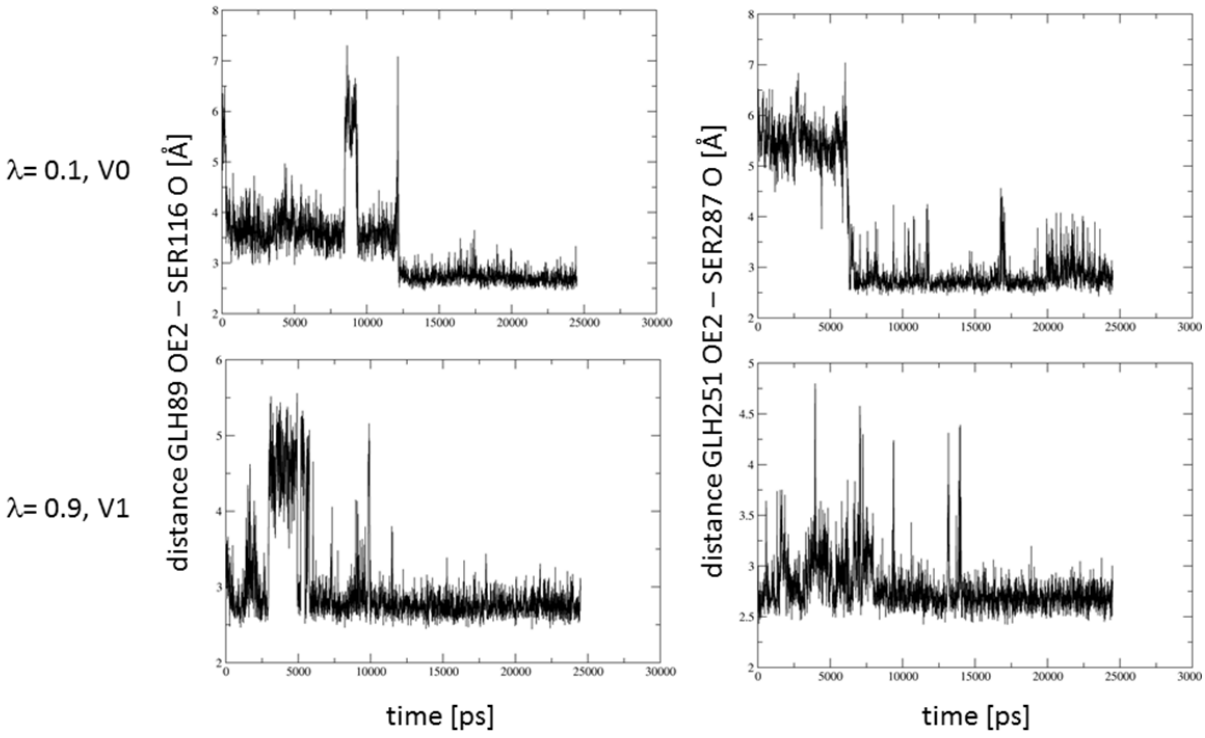

Figure S47. Distance between atoms OE2 of Glh89 and O of Ser116 for monomer 1 (left) and monomer 2 (Glh251 OE2-Ser287 O, right), indicating whether loop EF is closed by formation of a hydrogen bond between these atoms, vs. simulation time; data given for λ = 0.1 ("K^+-like") and λ = 0.9 ("Na^+-like"). "Bound" simulation (i.e., ions, protein and water present) of dimer.

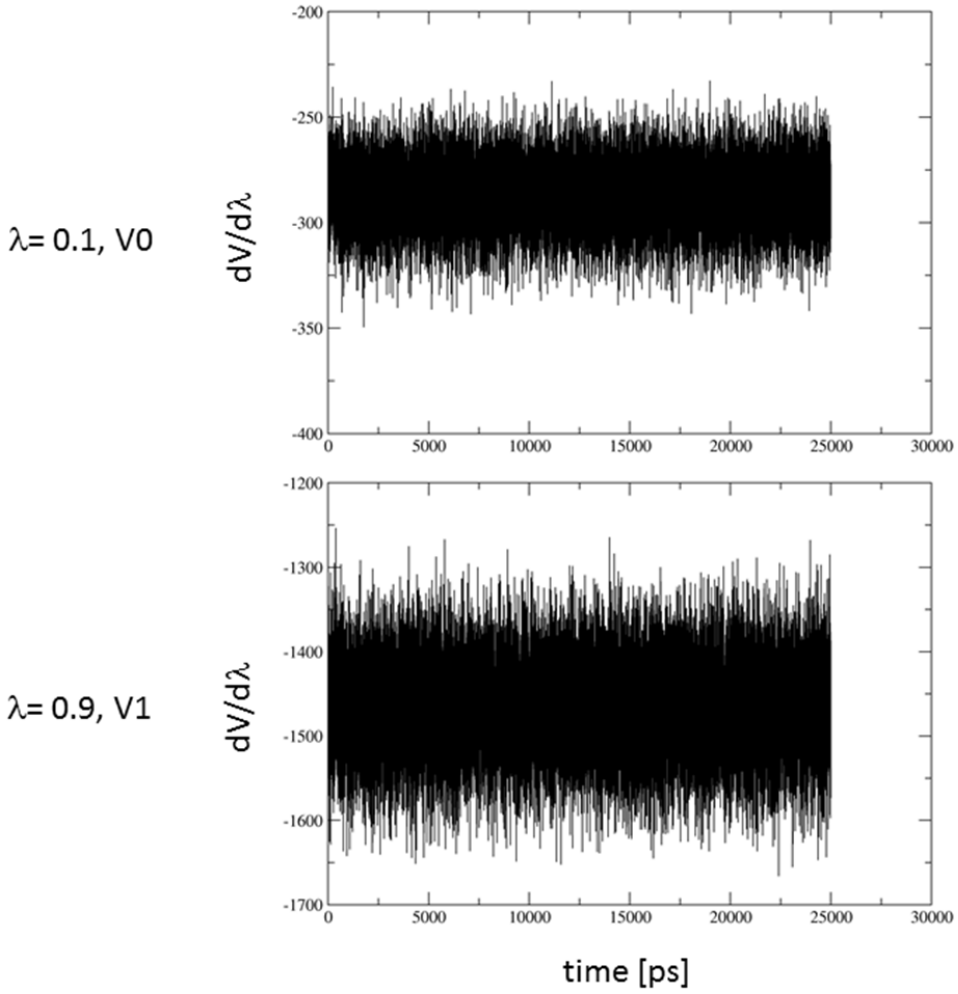

Figure S48. Gradients dV/dλ vs. simulation time, data given for λ = 0.1 ("K^+-like") and λ = 0.9 ("Na^+-like"). "Free" simulation (i.e., ions, and water present). Number of ions and water molecules as in dimer simulation.

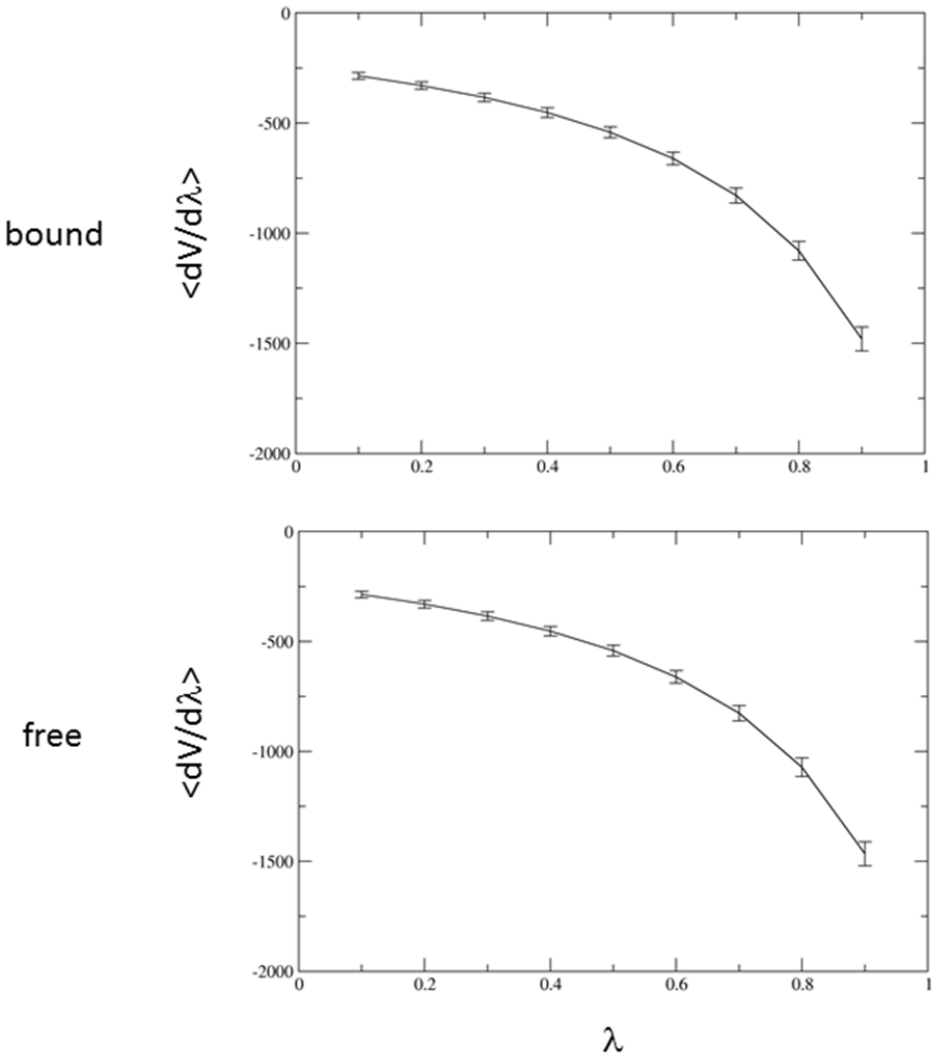

Figure S49. Ensemble averages of gradients <dV/dλ> vs. λ, data given exemplary for 24.5-25.0 ns. Dimer simulation.

Table S5. Integrated perturbation free energies, given for partial trajectories (0.5 ns each). SD: standard deviation, SE: standard error. "Bound" simulation (i.e., ions, protein and water present) of the dimer.

MD	time [ns]	ΔG_{pert} [kcal.mol^{-1}]
3	1.5	-712.31
4	2.0	-710.21
5	2.5	-709.23
6	3.0	-710.06
7	3.5	-709.39
8	4.0	-709.54
9	4.5	-710.22
10	5.0	-710.59
11	5.5	-709.88
12	6.0	-709.83
13	6.5	-709.67
14	7.0	-710.52
15	7.5	-710.45
16	8.0	-711.11
17	8.5	-710.28
18	9.0	-713.59
19	9.5	-708.45
20	10.0	-708.90
21	10.5	-710.25
22	11.0	-710.71
23	11.5	-710.29
24	12.0	-711.28

25	12.5	-710.46
26	13.0	-709.16
27	13.5	-709.00
28	14.0	-709.41
29	14.5	-709.72
30	15.0	-709.05
31	15.5	-708.92
32	16.0	-709.54
33	16.5	-709.98
34	17.0	-710.09
35	17.5	-709.74
36	18.0	-710.13
37	18.5	-711.21
38	19.0	-712.28
39	19.5	-709.53
40	20.0	-710.13
41	20.5	-709.82
42	21.0	-710.48
43	21.5	-709.47
44	22.0	-709.90
45	22.5	-709.75
46	23.0	-710.94
47	23.5	-710.14
48	24.0	-709.87
49	24.5	-709.99
50	25.0	-710.41
md11-50	mean	-710.11

SD	0.92
SE	0.14

Table S6. Integrated perturbation free energies, given for partial trajectories (0.5 ns each). SD: standard deviation, SE: standard error. "Free" simulation (i.e., ions, and water present). Number of ions and water molecules as in dimer simulation.

MD	time [ns]	ΔG_{pert} [kcal.mol^{-1}]
3	1.5	-707.07
4	2.0	-706.77
5	2.5	-707.53
6	3.0	-707.12
7	3.5	-707.53
8	4.0	-707.45
9	4.5	-707.69
10	5.0	-707.23
11	5.5	-706.91
12	6.0	-707.32
13	6.5	-706.98
14	7.0	-706.76
15	7.5	-707.43
16	8.0	-707.10
17	8.5	-707.11
18	9.0	-706.79
19	9.5	-707.00
20	10.0	-707.10
21	10.5	-707.08
22	11.0	-707.37
23	11.5	-706.85
24	12.0	-707.22

25	12.5	-707.47
26	13.0	-707.07
27	13.5	-707.26
28	14.0	-707.04
29	14.5	-707.48
30	15.0	-707.37
31	15.5	-707.59
32	16.0	-707.51
33	16.5	-707.44
34	17.0	-707.18
35	17.5	-707.08
36	18.0	-707.18
37	18.5	-707.20
38	19.0	-707.06
39	19.5	-707.50
40	20.0	-707.78
41	20.5	-706.82
42	21.0	-706.92
43	21.5	-707.45
44	22.0	-707.47
45	22.5	-707.07
46	23.0	-707.18
47	23.5	-707.07
48	24.0	-707.21
49	24.5	-707.16
50	25.0	-707.22
md11-50	mean	-707.19

SD	0.23
SE	0.04

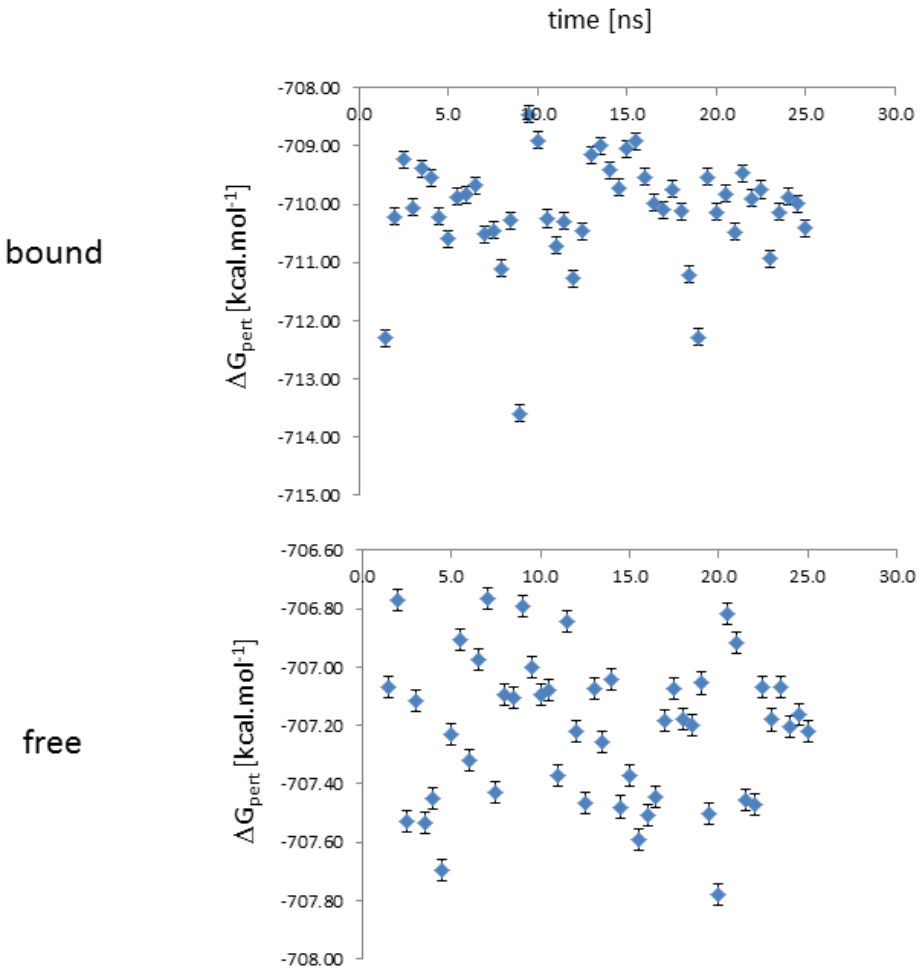

Figure S50. Integrated perturbation free energies, given for partial trajectories (0.5 ns each) vs. simulation time. Error bars are standard errors from batch averaging. Dimer simulation.

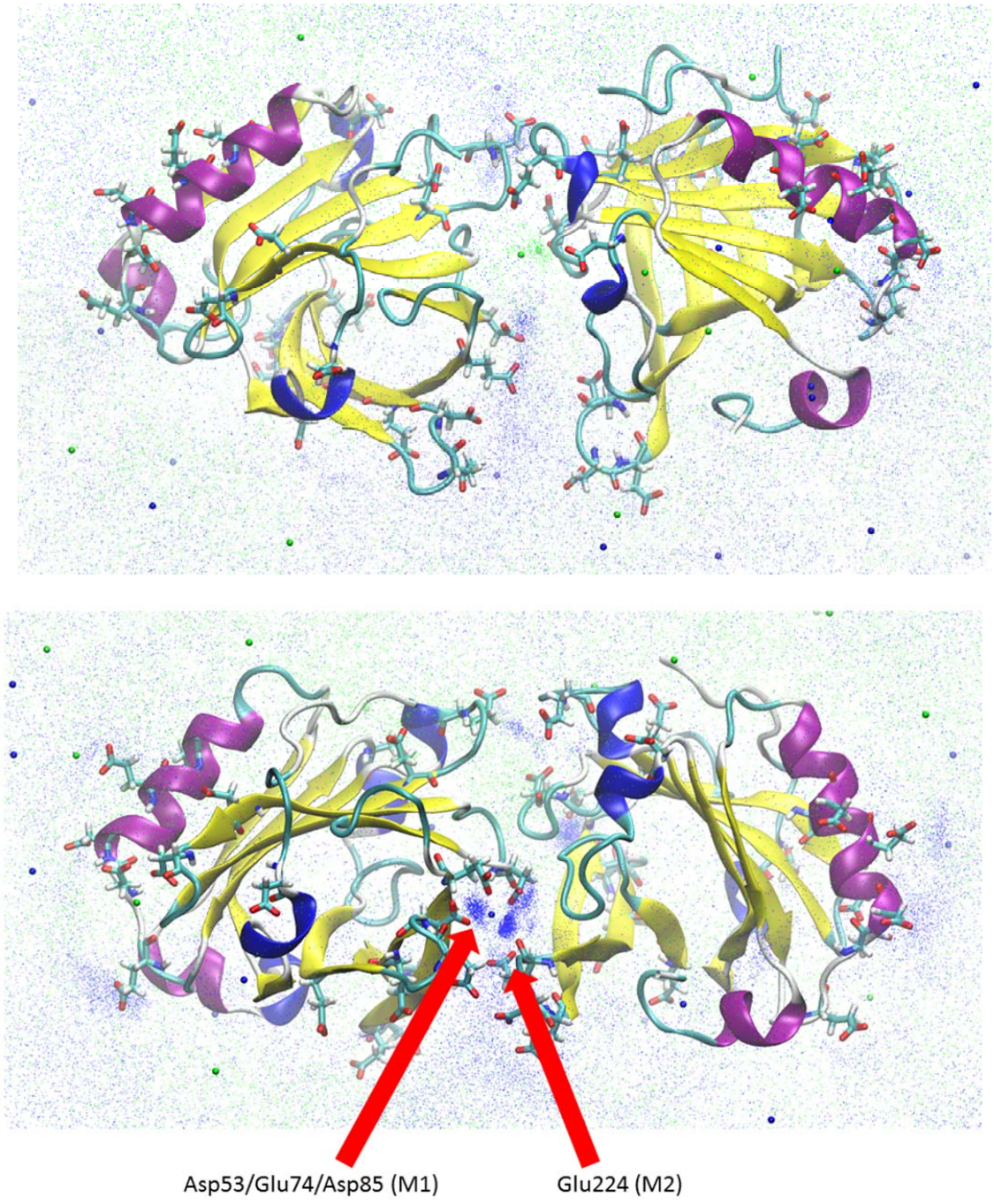

Figure S51. Structure of dimer after 25 ns (cartoon representation, Asp and Glu as sticks). Every structure of MCl in the time interval 5.0-25.0 ns shown. M^+: blue, Cl^-: green. Above: $\lambda = 0.1$ ("K^+-like"), below: $\lambda = 0.9$ ("Na^+-like"). Figures were created using VMD.[25,26]

Protein Diffusion Coefficients

Estimates for protein diffusion coefficients were determined from mean square displacements: In the monomer simulations, for the LiCl system, an interval from 10.5-100.5 ns was used and for the NaCl/KCl systems from 100.5-600.5 ns. For the dimer simulations, an interval from 101.5-209.5 ns was chosen. Mean square displacements versus time were calculated for the center of mass of all atoms (using a modified version of AmberTools ptraj provided by Hannes Loeffler),[27] and from these the diffusion coefficients were calculated using $D = \langle|\boldsymbol{r}(t) - \boldsymbol{r}(0)|^2\rangle/6t$. While the initial experimental data (dynamic light scattering) suggested faster protein diffusion in a KCl electrolyte compared to NaCl, and also a concentration dependence, our data do not show such an effect. The orders of magnitude of the calculated and the measured diffusion coefficients, however, agree well (approx. 2-3 $\cdot$ 10^{-7} cm^2 s^{-1} for the monomers, and approx. 0.3-1.2 $\cdot$ 10^{-7} cm^2 s^{-1} for the dimers). We are aware that a simulation in the NPT ensemble can only give a crude indication of the order of magnitude of protein diffusion coefficients, and that extensive sampling (e.g. by repeating the simulations with different starting velocities and extending simulation time) is required, as discussed in the literature.[28] It was shown in the literature that averaging mean square displacements from several simulation runs can help to obtain more accurate values for diffusion coefficients, even for large molecules like proteins.[28]

Table S7. Protein diffusion coefficients, monomer simulations, calculated from mean square displacements of the center of mass of all atoms.

	$D / 10^{-7}$ cm^2 s^{-1}
LiCl 100 mM	1.92
NaCl 20 mM	1.83
NaCl 100 mM	1.52
KCl 20 mM	2.18
KCl 100 mM	0.66

Table S8. Protein diffusion coefficients, dimer simulations, calculated from mean square displacements of the center of mass of all atoms.

dimer based on PDB code	loop	salt	$D / 10^{-7}$ cm^2 s^{-1}
2BLG	open	NaCl 100 mM	0.56
		KCl 100 mM	0.34
3BLG	closed	NaCl 100 mM	1.23
		KCl 100 mM	0.74

Coarse-Grain MD Simulations

For our coarse-grained (CG) MD simulations, we solvated 32 protein monomers (3BLG, protonation states as in the atomistic simulation) in ca. 800,000 water beads (representing 4 water molecules each), thus yielding a protein concentration of 547 μM, and added Na^+ and Cl^- beads (each representing a hydrated ion) to ensure an electrolyte concentration of 0.1 M. Parameters were taken from Martini 2.2, ion parameters (Na^+, Cl^-) from Martini 2.0.[29-31] All simulations were performed using Gromacs 4.x[32] on 32x12 CPUs (32x24 SMT cores), thus allowing to simulate ca. 1 μs/d. For the simulation parameters, standard Martini values were used (shifted cutoffs (LJ 0.9-1.2 nm, Coulomb 0.0-1.2 nm), ε_{rel} = 15, T-coupling: v-rescale, p-coupling: Parinello-Rahman, 30 fs integration step size, 300 K, periodic boundary conditions). The use of a cutoff for electrostatic interactions might be considered problematic as long-range interactions are neglected. However, Martini was parameterized to give optimal results using the above simulation parameters, and using a particle-mesh Ewald technique with Martini is currently still experimental and not sufficiently validated (although in principle possible with the polarizable variant of the force field).[31,33]

To study the aggregation and surface adsorption behavior of BLG, we performed 3 sets of coarse-grained (CG) MD simulations: First, a bulk system with evenly distributed BLG monomers was simulated. Additionally, 2 surface systems were set up. In one case, the protein monomers were evenly distributed in the aqueous phase in the starting structure, and in the other case, the protein monomers were initially placed near the surface. Each simulation was equilibrated for 333 ns and after that data were collected during 5.1 μs simulation. Simulations were performed in the NPT ensemble (bulk simulation) and in the NVT ensemble (surface systems, after NPT equilibration).

In the coarse-grained MD simulations, in all 3 scenarios (mostly linear) aggregates were quickly formed, and no clear surface preference was observed. An illustration is given in Figure S52. From the experimental results, however, we expect at least a monolayer of BLG at the surface for the pH value reflected by the protonation state of the protein. Possible reasons for the unsatisfactory performance of the CG force field are certainly the lack of atomic detail in the CG representation, the crude treatment of electrostatics and possibly the lack of orientational polarization in the water model. Also, the relatively high protein concentration in the simulation (compared to experiment) enhances aggregation. A further possible influence of the presence of the 100 mM NaCl electrolyte needs to be investigated. For future studies, using a polarizable model together with an improved description of electrostatics seems promising (Martini 2.2P).[31,33]

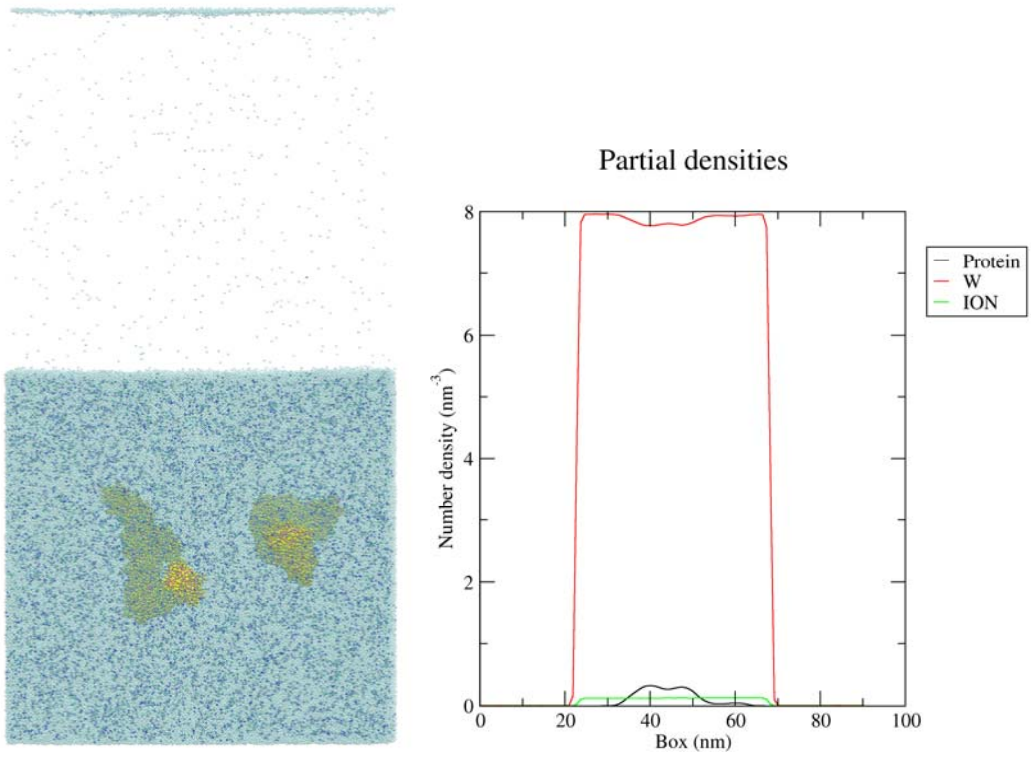

Figure S52. Left: Coarse-grained MD simulation of 32 BLGA monomers in a solution/vacuum system, snapshot after 5.433 μs. Right: particle density along the *z*-axis.

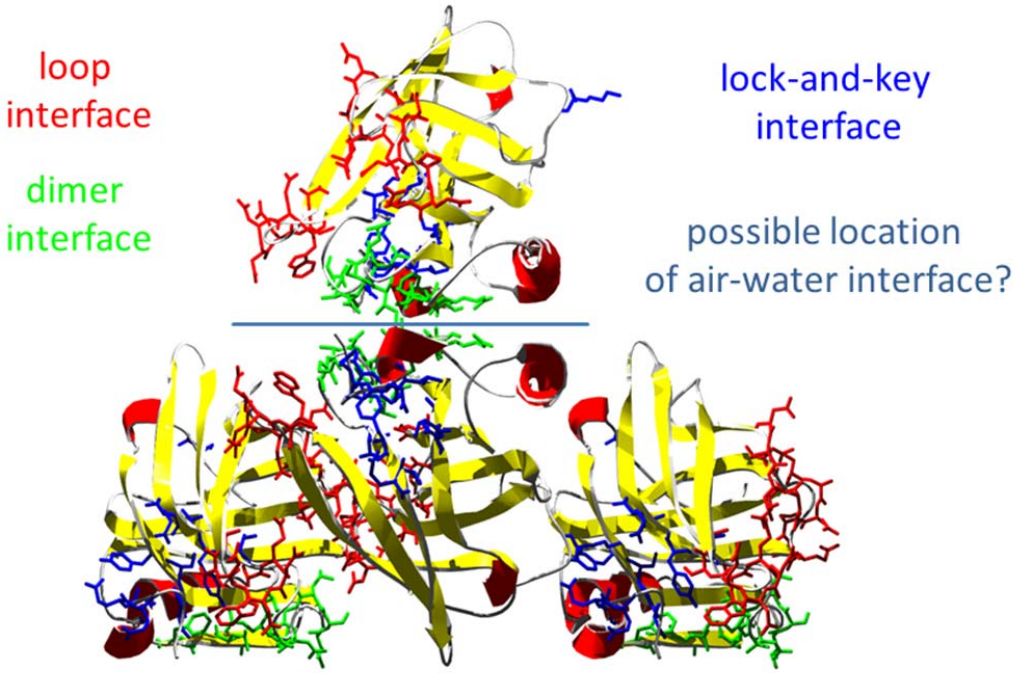

Figure S53. Four monomers, connected by the "lock-and-key", "dimer" and "loop" interfaces, based on PDB structure 3BLG.[1] Monomers in cartoon representation with residues forming contacts as colored sticks (blue: "lock-and-key", green: "dimer", red: "loop interface"). Images were created using Swiss-PDB-Viewer[2,3] and Pov-Ray.[4,5]

REFERENCES

1. Qin, B. Y.; Bewley, M. C.; Creamer, L. K.; Baker, H. M.; Baker, E. N.; Jameson, G. B. Structural Basis of the Tanford Transition of Bovine B-Lactoglobulin. *Biochemistry* **1998,** *37* (40), 14014-14023.
2. Swisspdb Viewer Web Page. http://www.expasy.org/spdbv/.
3. Guex, N.; Peitsch, M. C. Swiss-Model and the Swiss-Pdbviewer: An Environment for Comparative Protein Modeling. *Electrophoresis* **1997,** *18*, 2714-2723.
4. Pov-Ray Web Page. http://www.povray.org/.
5. *Persistence of Vision Raytracer (Version 3.6)*, Persistence of Vision Pty. Ltd., Williamstown, Victoria, Australia: 2004.
6. Tolkach, A.; Kulozik, U. Reaction Kinetic Pathway of Reversible and Irreversible Thermal Denaturation of ß-Lactoglobulin. *Lait* **2007,** *87* (4-5), 301-315.
7. Sauerbeck, C.; Braunschweig, B.; Peukert, W. Surface Charging and Interfacial Water Structure of Amphoteric Colloidal Particles. *J. Phys. Chem. C* **2014,** *118* (19), 10033–10042.
8. Engelhardt, K.; Lexis, M.; Gochev, G.; Konnerth, C.; Miller, R.; Willenbacher, N.; Peukert, W.; Braunschweig, B. Ph Effects on the Molecular Structure of B-Lactoglobulin Modified Air–Water Interfaces and Its Impact on Foam Rheology. *Langmuir* **2013,** *29* (37), 11646-11655.
9. Engelhardt, K.; Peukert, W.; Braunschweig, B. Vibrational Sum-Frequency Generation at Protein Modified Air-Water Interfaces: Effects of Molecular Structure and Surface Charging. *Curr. Opin. Colloid Interface Sci.* **2014,** *19* (3), 207-215.
10. Engelhardt, K.; Rumpel, A.; Walter, J.; Dombrowski, J.; Kulozik, U.; Braunschweig, B.; Peukert, W. Protein Adsorption at the Electrified Air–Water Interface: Implications on Foam Stability. *Langmuir* **2012,** *28* (20), 7780-7787.
11. Ryckaert, J.-P.; Ciccotti, G.; Berendsen, H. J. C. Numerical Integration of the Cartesian Equations of Motion of a System with Constraints: Molecular Dynamics of N-Alkanes. *J. Comput. Phys.* **1977,** *23* (3), 327-341.
12. Darden, T.; York, D.; Pedersen, L. Particle Mesh Ewald: An N Log(N) Method for Ewald Sums in Large Systems. *J. Chem. Phys.* **1993,** *98*, 10089-10092.
13. Essmann, U.; Perera, L.; Berkowitz, M. L.; Darden, T.; Lee, H.; Pedersen, L. G. A Smooth Particle Mesh Ewald Method. *J. Chem. Phys.* **1995,** *103*, 8577-8593.
14. Case, D. A.; Darden, T. A.; Cheatham III, T. E.; Simmerling, C. L.; Wang, J.; Duke, R. E.; Luo, R.; Walker, R. C.; Zhang, W.; Merz, K. M., et al. *Amber 12*, University of California, San Francisco: 2012.
15. Roe, D. R.; Cheatham, T. E. Ptraj and Cpptraj: Software for Processing and Analysis of Molecular Dynamics Trajectory Data. *J. Chem. Theory Comput.* **2013,** *9* (7), 3084-3095.
16. Case, D. A.; Babin, V.; Berryman, J. T.; Betz, R. M.; Cai, Q.; Cerutti, D. S.; Cheatham III, T. E.; Darden, T. A.; Duke, R. E.; Gohlke, H., et al. *Amber 14*, University of California, San Francisco: 2014.
17. Jäger, C. M.; Hirsch, A.; Schade, B.; Ludwig, K.; Böttcher, C.; Clark, T. Self-Assembly of Structurally Persistent Micelles Is Controlled by Specific-Ion Effects and Hydrophobic Guests. *Langmuir* **2010,** *26* (13), 10460-10466.
18. Jäger, C. M.; Hirsch, A.; Schade, B.; Böttcher, C.; Clark, T. Counterions Control the Self-Assembly of Structurally Persistent Micelles: Theoretical Prediction and Experimental Observation of Stabilization by Sodium Ions. *Chem. Eur. J.* **2009,** *15* (34), 8586-8592.

19. Rosenlehner, K.; Schade, B.; Böttcher, C.; Jäger, C. M.; Clark, T.; Heinemann, F. W.; Hirsch, A. Sodium Effect on Self-Organization of Amphiphilic Carboxylates: Formation of Structured Micelles and Superlattices. *Chem. Eur. J.* **2010,** *16* (31), 9544-9554.
20. Berendsen, H. J. C.; Grigera, J. R.; Straatsma, T. P. The Missing Term in Effective Pair Potentials. *J. Phys. Chem.* **1987,** *91* (24), 6269-6271.
21. Joung, I. S.; Cheatham III, T. E. Determination of Alkali and Halide Monovalent Ion Parameters for Use in Explicitly Solvated Biomolecular Simulations. *J. Phys. Chem. B* **2008,** *112* (30), 9020-9041.
22. Horinek, D.; Mamatkulov, S. I.; Netz, R. R. Rational Design of Ion Force Fields Based on Thermodynamic Solvation Properties. *J. Chem. Phys.* **2009,** *130* (12), 124507.
23. Tutorial A9, Amber Web Site. http://ambermd.org/tutorials/advanced/tutorial9/.
24. Beierlein, F. R.; Kneale, G. G.; Clark, T. Predicting the Effects of Basepair Mutations in DNA-Protein Complexes by Thermodynamic Integration. *Biophys. J.* **2011,** *101* (5), 1130-1138.
25. Humphrey, W.; Dalke, A.; Schulten, K. Vmd - Visual Molecular Dynamics. *J. Molec. Graphics* **1996,** *14*, 33-38.
26. Vmd Web Page. http://www.ks.uiuc.edu/Research/vmd/.
27. Loeffler, H. Handy Routines for Ptraj/Cpptraj. Science and Technology Facilities Council Daresbury Laboratory Web Page. http://www.stfc.ac.uk/cse/25249.aspx.
28. Wang, J.; Hou, T. Application of Molecular Dynamics Simulations in Molecular Property Prediction Ii: Diffusion Coefficient. *J. Comput. Chem.* **2011,** *32* (16), 3505-3519.
29. Marrink, S. J.; Risselada, H. J.; Yefimov, S.; Tieleman, D. P.; de Vries, A. H. The Martini Force Field: Coarse Grained Model for Biomolecular Simulations. *J. Phys. Chem. B* **2007,** *111* (27), 7812-7824.
30. Monticelli, L.; Kandasamy, S. K.; Periole, X.; Larson, R. G.; Tieleman, D. P.; Marrink, S.-J. The Martini Coarse-Grained Force Field: Extension to Proteins. *J. Chem. Theory Comput.* **2008,** *4* (5), 819-834.
31. de Jong, D. H.; Singh, G.; Bennett, W. F. D.; Arnarez, C.; Wassenaar, T. A.; Schäfer, L. V.; Periole, X.; Tieleman, D. P.; Marrink, S. J. Improved Parameters for the Martini Coarse-Grained Protein Force Field. *J. Chem. Theory Comput.* **2013,** *9* (1), 687-697.
32. Gromacs Web Page. http://www.gromacs.org/.
33. Yesylevskyy, S. O.; Schäfer, L. V.; Sengupta, D.; Marrink, S. J. Polarizable Water Model for the Coarse-Grained Martini Force Field. *PLoS Comput Biol* **2010,** *6* (6), e1000810.